Atmosphere

Volume 14 Number 1 1976

anadian Meteorological Society
ociété Météorologique du Canada

Atmosphere

Volume 14 Number 1 1976

Contents

ISSN 0004–6973

Canadian Meteorological Socie
Société Météorologique du Cana

The General Circulation of the Pacific Ocean and a Brief Account of the Oceanographic Structure of the North Pacific Ocean[1] Part II – Thermal Regime and Influence on the Climate[2]

S. Tabata

Institute of Ocean Sciences, Patricia Bay, Environment Canada, 1230 Government Street, Victoria, B.C.

[Manuscript received 29 September 1975]

ABSTRACT

The main features of sea-surface temperature distribution are described and it is noted that most deviations of the isotherms from a zonal orientation are the result of advective and convective effects. In the Subarctic region the salinity structure of the upper layer determines the depth of convective overturn whereas in the Subtropic region it is determined by the thermal structure. From a standpoint of large-scale atmosphere-ocean interaction, the equatorial region appears to be of primary importance. Some recent studies, for example, show that the sea temperature anomalies in this region could well influence climate in the middle and higher latitudes as well as in the lower latitudes. A suggestion is made as to which areas of the Pacific Ocean could benefit from an intensive study.

9 Heat transport by ocean currents

Up to now I have made very few comments about the ocean that are likely to interest many meteorologists. However, a certain amount of background information on currents and transports is a prerequisite to the understanding of the heat transport by ocean currents – which is of interest to them! As is evident from the preceding section our knowledge of the water volume transport is still very incomplete. Even the estimated volume transports given are based on results that employ dissimilar methods, thereby making a meaningful comparison of transports difficult. Our knowledge concerning the transport of heat by ocean currents in the Pacific Ocean and elsewhere is disappointingly poor indeed. I shall attempt to make references to the few studies that have been made in the past for the North Pacific Ocean only, as no study has been made for the South Pacific Ocean. An early estimate of the heat transport in the North Pacific indicated that the mean oceanic heat transport was poleward and was, on the average, only 10% of that transported by the atmosphere (Sverdrup, 1957; Houghton, 1954). Hence it was considered that the North Pacific Ocean was not an effective transporter of heat from the equatorial region poleward. However, the heat budget studies by Pattullo (1957) and Wyrtki (1965) both indicated that there was a net influx of heat from the atmosphere

[1]Invited lecture for the 9th CMS Congress, Vancouver, B.C., 27–29 May 1975.
[2]For part I see Atmosphere **13**, 133–168.

to the ocean in the region north of the Equator, the former giving an estimated heat gain of 1.0×10^{19} g-cal/day and the latter, of 2.6×10^{19} g-cal/day. Further, Bryan (1962), using the NORPAC data of August 1955 (NORPAC Committee, 1960), and considering the geostrophic transport values as well as using the heat-balance maps compiled by Budyko (1956) and Albrecht (1960), estimated that there was an equatorward transport of heat equivalent to 1.8×10^{19} g-cal/day at latitude 32°N. Since Bryan's estimate is for a particular latitudinal belt and since the transport values were for August 1955, his result is not expected to represent an annual average and is probably fortuitous. Even at Station P (50°N, 145°W) there appears to be a net annual heat gain (Tabata, 1965), although here it is possible to overcome the heat surplus by loss of heat through upwelling of cold water and by advection of cold water. Although both Bryan (1962) and Wyrtki (1965) proposed that the heat is transported equatorward, the former considers that this can occur in the upper 1500 m depth while the latter believes that this occurs mainly in the upper layers above the thermocline and that the heat surplus is balanced by a circulation in the meridional plane involving ascending movement of the water.

The earlier estimates by Sverdrup (1957), together with the early and more recent numerical models of the ocean-atmosphere climatic models (Bryan, 1969; Manabe, 1969; Bryan *et al.*, 1975; Manabe *et al.*, 1975), all indicate a net poleward transport of heat. Further, Vonder Haar and Oort (1973), using an improved estimate of the radiative flux values from satellite observations, have re-estimated the heat flux into the ocean and have concluded that the net oceanic heat transport is indeed poleward and much greater than had previously been determined. They added that in the region of the maximum net transport by the ocean-atmosphere system, between 30° and 35°N, the ocean transports almost half as much (4.7×10^{19} g-cal/day) as the atmosphere and that at 20°N as much as ¾ of the atmosphere poleward heat transport. This means that the relative importance of the ocean in the transport of heat has been vastly increased.

Jung (1952), in a earlier study of the heat transport of the Atlantic Ocean, suggested the possible importance of considering the meridional circulation in the vertical plane in order to obtain the proper estimate of the heat transport. This has further been voiced by Bryan (1962), who points out that the mean currents in the vertical plane, though relatively slower than those in the upper layers, may dominate heat transport in the oceans. In the Subarctic region the upper Ekman layers of the ocean are divergent and therefore we can assume that any surplus heat may be neutralized, at least partly, by the upward movement of cold deep water, as has been proposed for Station P. However, the Ekman layer in the Subtropic region is convergent and we cannot assume upwelling of cold, deep water there. Thus, if in this area there is still an incoming surplus heat, some other type of influx of cold water, other than due to upwelling, needs to be involved. In the Pacific Ocean there is an inflow of cold, deep water originating in the Antarctic Ocean which flows northward, as mentioned earlier, and it is possible that if a sufficient amount of this flow enters

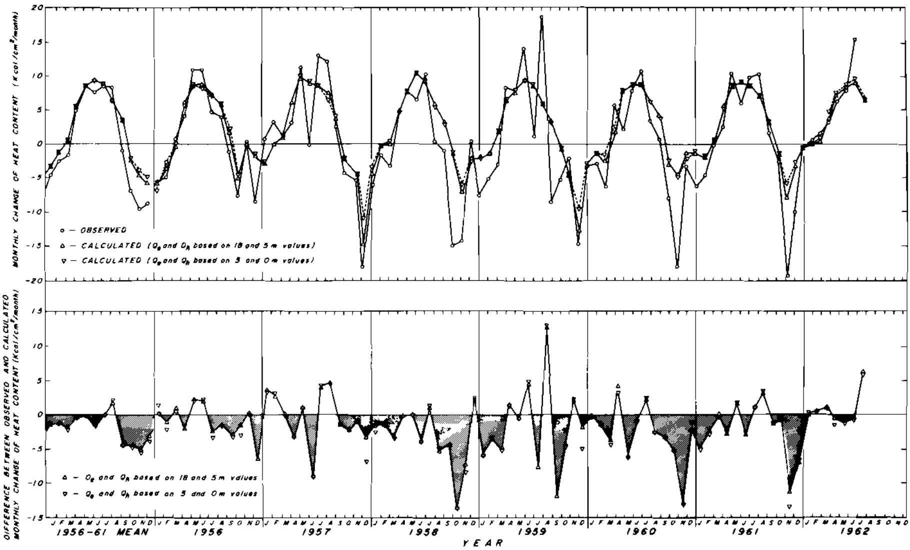

Fig. 12 Comparison of the observed change of heat content in the upper 120 m of water at Ocean Station *P* (50°N, 145°W) with the calculated heat flux across the air-sea boundary (kcal.cm^{-2}/month).

the North Pacific the surplus heat could be balanced out. But this would probably require a much larger northward transport of deep water than has been estimated. Hence, it may be necessary to propose a northward transport at some intermediate levels as well.

The overall heat transport in the North Pacific must be equatorward and it is difficult to imagine it otherwise. So if the advective and convective effects in the ocean cannot balance the heat surplus that appears to occur, it must be concluded that the surplus incoming heat flux into the ocean might be overestimated.

10 Distribution of sea surface temperature

In the absence of advective and convective effects in the ocean, caused by the large-scale horizontal and vertical transport respectively, the temperature of the ocean will be governed primarily by the heat exchange occurring across the atmosphere-ocean boundary. At Station P in the Northeast Pacific Ocean (Tabata, 1965) and elsewhere where advective effects are relatively small, but away from the tropical zone (Gill and Niiler, 1973), the temperature of the upper layers of the ocean varies in direct response to the heat input. An example of this is shown in Fig. 12. This illustration does, however, suggest that during the autumn and winter advective effects could be appreciable. If the heat exchange across the air-sea boundary alone is important, the isotherms would extend zonally across the ocean and would show a gradual decrease from the equatorial to the polar regions. But the observed distribution of temperatures in the upper layers of the ocean is never this simple. A few illustrations will be shown to exemplify this.

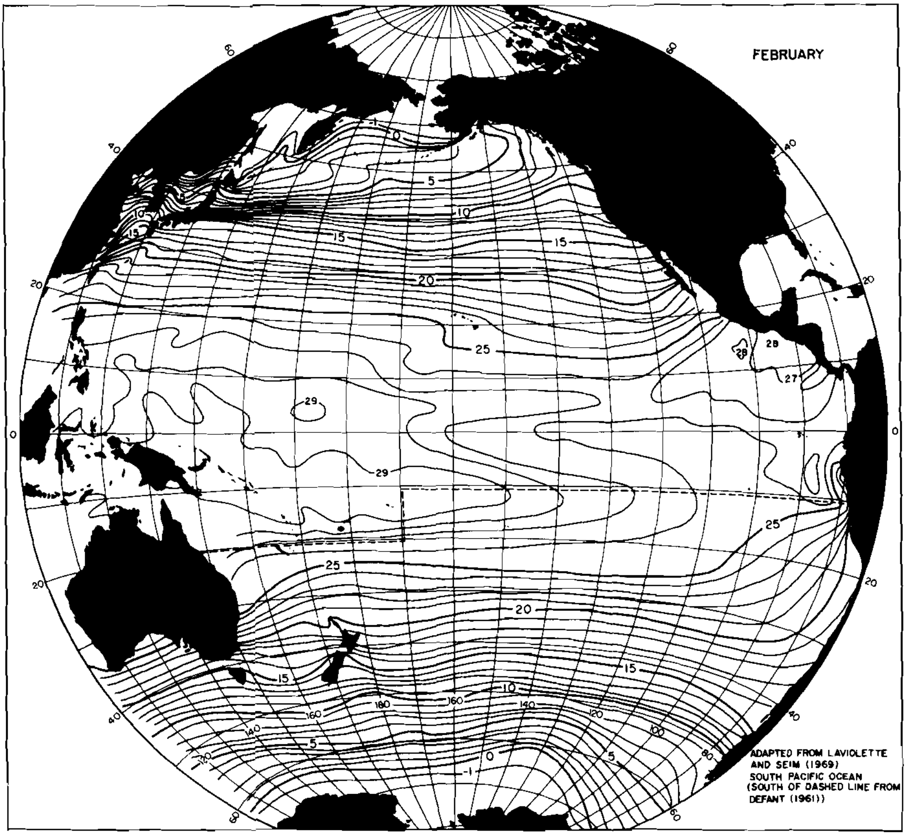

Fig. 13 (a) February. Average sea surface temperature (°C) for the Pacific Ocean. The temperatures for the North Pacific and the Equatorial South Pacific are based on charts prepared by Laviolette and Seim, 1969, while those for the most of the South Pacific are based on charts prepared by Defant, 1961, which are likely to be based on data collected prior to 1940.

Fig. 13a shows the average winter (February) sea surface temperatures for the Pacific Ocean. As with the distribution of sea surface temperatures at other times over the world ocean this figure is practically all based on data obtained by merchant ships, again emphasizing the large contribution they have made to oceanography. When the distribution of sea surface temperatures of the North Pacific and equatorial belt based on earlier data are compared with those based on more recent data, the general distribution of temperature depicted in both distributions are found to be similar with one exception – the recent chart shows that the equatorial belt is approximately 1°C warmer than the earlier one but it is not known whether this increase is statistically significant or not.

It is evident from the distribution shown in this figure that the isotherms occur more or less zonally but not quite so. In the North Pacific, north of 40°N they are shifted poleward along the eastern side and slightly equatorward on the western side, but south of 40°N they are shifted in the opposite direction,

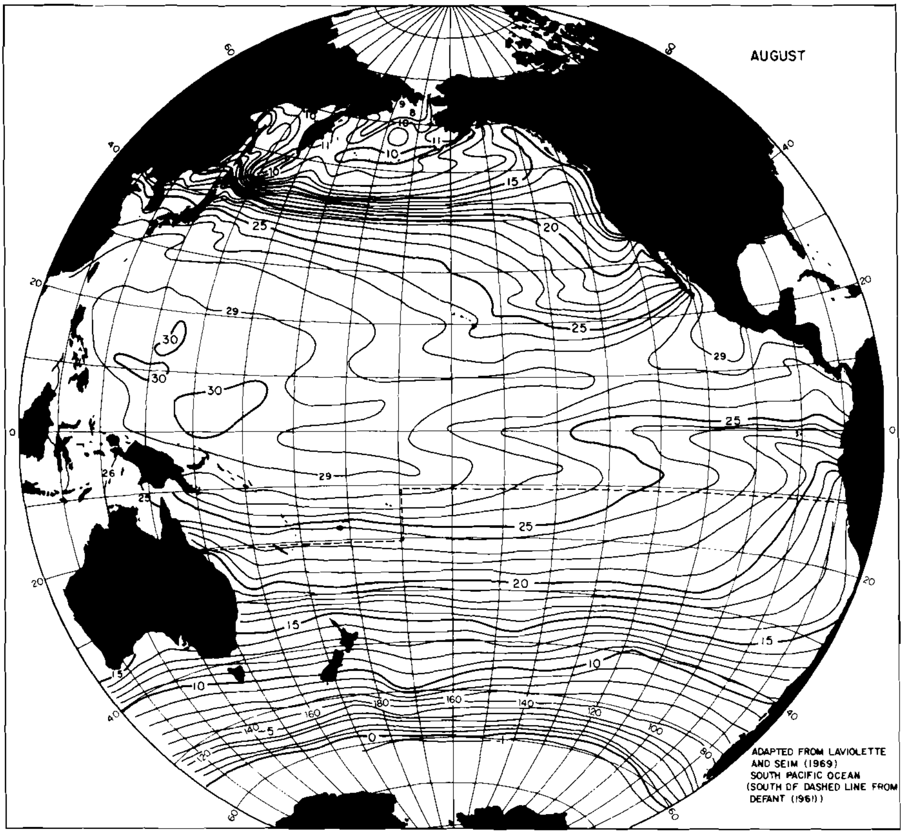

Fig. 13 (b) August. Average sea surface temperature (°C) for the Pacific Ocean. The temperatures for the North Pacific and the Equatorial South Pacific are based on charts prepared by Laviolette and Seim, 1969, while those for the most of the South Pacific are based on charts prepared by Defant, 1961, which are likely to be based on data collected prior to 1940.

equatorward along the eastern side and poleward along the western side. Similar shifts are evident in the South Pacific except that the shifts along the western and eastern sides are more pronounced than in the North Pacific as indicated by the 25°C isotherms. There are other features of the distribution. For example, the warmest water in the equatorial belt is along the western side, and here the water is warmer to the south of the Equator while it is warmer to the north on the eastern side. Also, the eastern part of the Equator is characterized by a belt of relatively cool water. Moreover, between 30° and 40° in both oceans the isotherms are more closely spaced along the western than on the eastern side of the ocean, particularly off Japan; the isotherms diverge in the temperate latitudes along the eastern side in both the North and South Pacific. Finally, a body of cool water is present off the coast of Northern Peru (to the South of the Equator) and off Guatemala (to the north of the Equator); a belt of warm water occurs between the Equator and 10°N along the eastern end of the equatorial belt. Along the western end of the equatorial belt the body of warm water is centred along 10°S and extends well along the western side of the ocean.

We shall attempt to explain the occurrence of these features by a qualitative consideration of the advective and convective effects. The presence of the warmer water along the western end of the equatorial belt is probably due to the westward drift of water produced by the Trade Winds, while the occurrence of the warmer water to the south of the Equator can be attributed to the general southward-blowing winds during the northern winter. The presence of the cooler water along the eastern end is partly due to the intrusion of colder water carried equatorward by the Peru current and partly due to the upwelling caused by the southerly winds that blow along the Pacific coast of South America and the northerly winds that blow along the west coast of Central America. The occurrence of cold water along the northern coast of Peru is no doubt associated with the upwelling induced by the offshore Ekman transports. The poleward shift of the isotherms along the western end of the tropical and subtropical regions is attributed to the poleward flowing currents while the equatorial shift along the eastern side is attributed to the equatorward flow of the currents. The marked north-south gradient of temperature off the coast of Japan can be explained by the fact that the poleward-flowing warm Kuroshio water meets the cold equatorward-flowing waters of the Oyashio in this region. The poleward shift in the isotherms in the temperate latitudes along the eastern side is attributable to the wind-driven circulation that results in transport of warmer water poleward.

In Fig. 13b the distribution of the average surface sea temperature for the summer (August) is shown. As was the case for the winter distribution, the earlier charts show that the distribution for the North Pacific and the equatorial belt is similar to the recent one, except that the recent chart again shows that the water in the equatorial belt and the tropical region is about 1 °C warmer than indicated in the earlier distribution. Although the gross features of the pattern of sea surface temperature distribution for the two seasons are alike, there are recognizable differences in addition to the obvious changes caused by the seasonal variations in the heat flux across the atmosphere-ocean interface. Again, as was the case for the winter, the western sides of the equatorial and tropical regions are warmer than along the eastern side. But in contrast to the winter condition, the warmest water is found to the north of the Equator along the western side as well as along the eastern side. The presence of the warmer water along the western side can again be related to the effect of the westward transport of water along the equatorial belt and also to the fact that the eastern side is kept cooler by the effect of upwelling. The reason, however, for the presence of a warmer water north of the Equator is uncertain. Perhaps it is due to the increased strength of the Southeast Trades that occur along the western side during this time. The equatorial belt is again characterized by the presence of cooler water which, during this time, extends further to the west. While the equatorward shift in the isotherms is perhaps even more marked than during the winter along the eastern side, the poleward shift along the western side is only evident in the North Pacific. In fact in the South Pacific the shift, which is evident only off the eastern coast of Australia, is equatorward. The marked shift of the isotherms in the North Pacific is probably related to the shift of winds, for during the summer the winds are southerly along the western side and northerly along the eastern side. The occurrence of cold water along the coast of North America is no doubt due to the effect of upwelling resulting from the offshore Ekman transport. The presence of a tongue of relatively warm water some distance away from the coast of British Columbia rather than along the coast is due to the modifying influence of coastal upwelling upon the poleward transport of warm water in the region.

The tongue-like distribution of warm-water off Japan is likely due to the poleward transport by the Kuroshio, and a similar tongue lying in the vicinity of the Hawaiian Islands is probably formed as the California and North Pacific Currents feed into the North Equatorial Current. The reason for the occurrence of a body of warm water off Guatemala is unclear. It is probably due to the failure of the California Current to extend this far and to the absence of a northward extension of equatorial upwelling. There might possibly also be other explanations for its occurrence. The marked equatorward shift of the isotherms to the west of the South American coast is likely to be associated with the northward transport of cooler water from the south by the Peru Current. Similarly, the equatorward shift of the isotherms off the west coast of the United States is due to the advective effects of the California and North Pacific Currents. Although the presence of cooler water along the Equator is attributed to the effect of upwelling, there is also the possibility of this cooling to be due partly to the intrusion of the cold water from the South. But whether or not this cold water can have an influence so far north is uncertain. The winds along the Pacific coast of South America are from the south during the summer as well as in winter and can therefore cause upwelling throughout the year. Thus the appearance of the cold water along this coast is also likely to be associated with upwelling. The equatorward shift of isotherms in the vicinity of the northern Pacific side of Australia is probably produced by the southerly winds that occur during the southern winter.

The distribution of sea surface temperature discussed above is based on average conditions based on many years of observations. No doubt, there will be appreciable variations of the temperatures at the various locations from one period to another. The year-to-year and other long-term changes of temperatures can be attributed to the corresponding changes in the heat flux across the atmosphere-ocean interface. However, it is evident from the foregoing discussion that changes in the horizontal transport could contribute to significant temperature changes. Moreover, such changes could also result from changes in the intensity of convective mixing which will be discussed subsequently.

Intense interest in the anomalies of sea surface temperatures began after the sequence of extraordinary events that took place in the Pacific Ocean during 1957–1958. Widespread warming of the ocean occurred along the Pacific coast of North and South America and was evident further offshore to at least the location of Station P. Elsewhere in the Pacific other dramatic events occurred: *El Niño* occurred along the South America coast (*El Niño* is associated with the intrusion of warm water off the coast of Ecuador and Peru occurring at intervals varying from 4 to 14 years); the area off Point Barrow, Alaska was ice-free at the earliest time in its history; in the countries along the western side of the Pacific rim, the tropical rainy season lasted six weeks beyond its usual period; Hawaii recorded its first typhoon (California Department of Fish and Game, Marine Research Committee, 1960); the migration route of salmon returning to the usual spawning river changed; larger numbers of pelagic warm-water species of fish were found along the coast of Oregon, Washington and British Columbia. As is shown in Fig. 14, the anomalies of monthly mean sea surface temperatures recorded from a station along the British Columbia coast and at Station P (based on 22-year means (1950-1971)) indicated a pronounced warming along the eastern side of the Pacific Ocean. Similar anomalies were present in the early 1940's and in 1963 along the coast. At Station P, some degree of warming is present in 1972 as well. It is interesting to note that warming also occurred along the South American coast in the early 1940's, in 1965 and in 1972 (Ramage *ibid.*) but not in 1963, although at other parts in the mid-Pacific equatorial region warming in 1963 was evident (Bjerknes, 1969). The finding that lower temperatures along the eastern side of the North Pacific during 1950, 1952, 1954 through 1956 are reflected in the coastal temperatures of South America, leads one to conclude that the anomalies are probably caused by large-scale global events. It has been shown by Uda (1967) and more recently by Favorite and McClain (1973) that these warm anomalies in the North Pacific migrate eastward. For example, they were first detected along the western North Pacific in 1955 and then finally appeared along the coast of North America in 1957–58. At Station P the 1957–58 warming was not only evident at the sea-surface but also occurred in the upper few hundred metres (Tabata, 1965).

Subsequent to the 1957–58 warming, anomalies of monthly mean sea surface temperature of the eastern North Pacific and the equatorial region have been prepared regularly. In addition, since June 1973 much of the area of the North Pacific and equatorial regions of the eastern South Pacific are compiled and distributed by NOAA (Eber and Miller, 1974). An example of the latter is shown in Fig. 15 for the month of August 1974. In this illustration the largest anomalies are 2°C. In other years anomalies as large as 4°C have been noted to occur in the equatorial region. The main feature of the anomalies shown is that they generally occur over relatively large areas. For example, the negative anomalies stretch from an area off the California Peninsula to the equatorial area some distance south of the Hawaiian Islands. Sandwiched between the two negative anomalies is a broad belt of positive anomalies, with maximum positive temperature anomaly lying in an area just south of the Hawaiian Islands. The largest positive anomaly occurs in a small area along the coast of Colombia. Examination of similar charts containing these anomalies

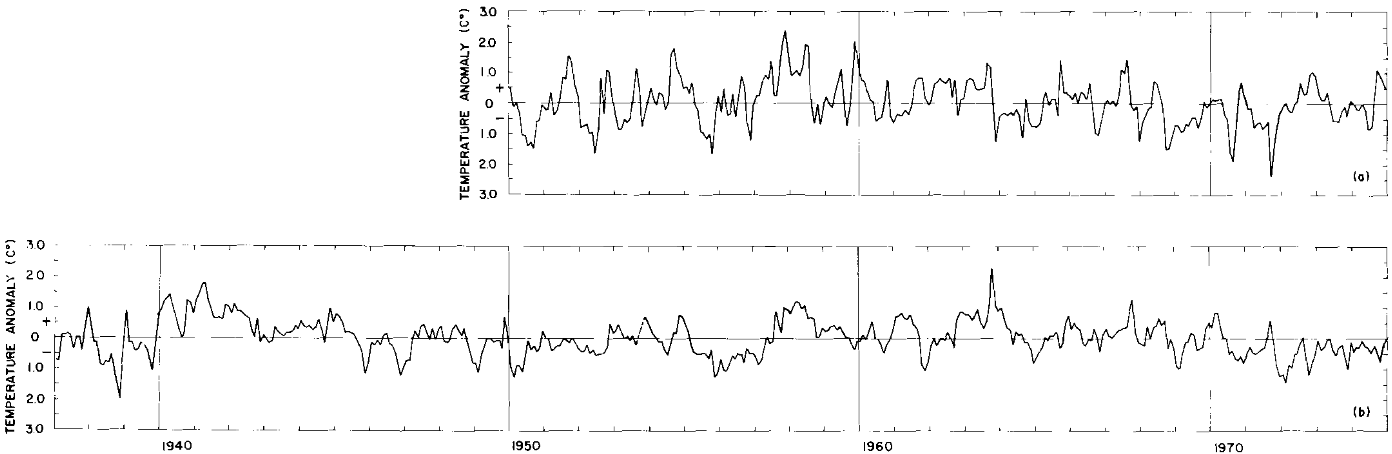

Fig. 14 Anomaly of monthly sea surface temperature (°C) based on 22-year means – 1950–1971.
(a) Station *P* (50°N, 145°W)
(b) Pine Island – Northern tip of Vancouver Island.

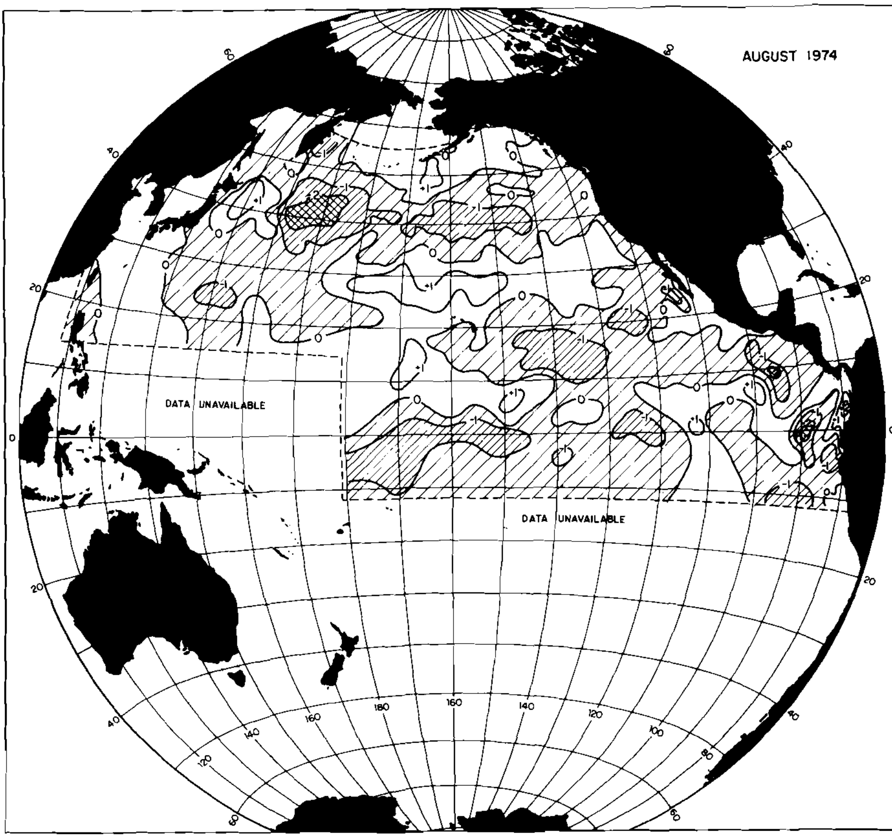

Fig. 15 Anomaly of monthly temperature (°C) for the month of August 1974 based on 20-year averages (1948–1967) for the North Pacific and Equatorial Pacific (Adapted from Eber and Miller, 1974).

indicates that some of them will persist for several months while others are short-lived.

The extrapolation of sea surface temperature anomalies from one region to another may be misleading if too much extrapolation is made. For example, the small positive anomaly noted for Station P (Fig. 14) is part of a larger area to the north and west of Station P which has not yet reached the coast. Therefore, use of coastal sea surface anomalies to reflect the open area conditions of the offshore region could be quite dangerous.

The anomalies of monthly mean sea surface temperatures are now compiled regularly so that it is possible to utilize them for monitoring or for predictive purposes. However, up until recently the only locations where the oceanic properties in the deeper layers were observed routinely in the North Pacific were at the Ocean Weather Stations. Now there is only one, Station P, that makes year-long observations. Analysis of the thermal structures in the upper few hundred metres of the ocean at Station P (50°N, 145°W), Station V

(34°N, 164°E) and Station N (30°N, 140°W) have indicted that, at Station P and Station N, the anomalous temperatures at the surface led in time to similar anomalies in the deeper levels. At Station V, on the other hand, downward propagation from the surface was absent (White and Walker, 1974). Their analysis also indicated that during much of the decade of the 1950's the anomaly developments at the three stations were well correlated with one another. During 1954 to 1961 the anomalous thermal structures at Station P and Station N fluctuated in phase with each other but were out of phase with the structures at Station V. During the decades of the 1960's the ordered relationship disappeared completely. Such relationships or non-relationships are not unexpected, however, as the three stations are located some distance away from one another. Moreover, it can be expected that some large-scale events may influence the conditions at all stations, while a smaller scale event would only influence the conditions at one or two of the stations.

How effective these sea surface temperatures are to the overlying atmosphere will probably depend on how persistent the anomalies are with depth. Clearly, a "thick" positive anomaly can have in storage a greater amount of heat than a thinner one. The bulk of the heat available for the overlying atmosphere is generally contained within only the upper 100 m or so of the surface. Since most of the heat entering the ocean is stored during the heating season in this layer, the processes governing the changes in the thermal structures in the upper few hundred metres will be important to the study of the interaction between the atmosphere and the ocean.

For the remainder of the discussion we shall only use information obtained from the Subarctic and Subtropical region as more data are available from there. It will not be unreasonable to assume that similar processes governing changes of the thermal structures in the North Pacific should be applicable to the corresponding regions of the South Pacific.

There are two main oceanic regions north of the equatorial belt – the Subarctic Pacific region and the Subtropic Pacific region. The so-called Subarctic Boundary separating these two regions is located at about 40°N over most of the North Pacific and lies close to the great circle route between San Francisco, U.S.A. and Yokohama, Japan. The Subarctic region is featured by the presence of relatively cool water and a surface layer whose salinity is relatively low at the surface (precipitation exceeds evaporation). It possesses a distinct halocline between depths of 100–200 m in which the salinity increases markedly with depth. Below this, the salinity increases with depth more gradually as shown in Fig. 16a. During the summer a secondary halocline is present at a depth of between 30 m and 50 m. While the upper 100 m of the water column here is isothermal in winter, a noticeable increase in the temperature takes place during the warming season and a marked thermocline forms at the depths of the secondary halocline. Below this the temperature decreases gradually with depth. It is possible that the upper layer of the ocean here can get colder than the water in the 100–200 m level when intensive cooling occurs during the winter. In Fig. 16a, the temperature is shown to decrease with depth in the

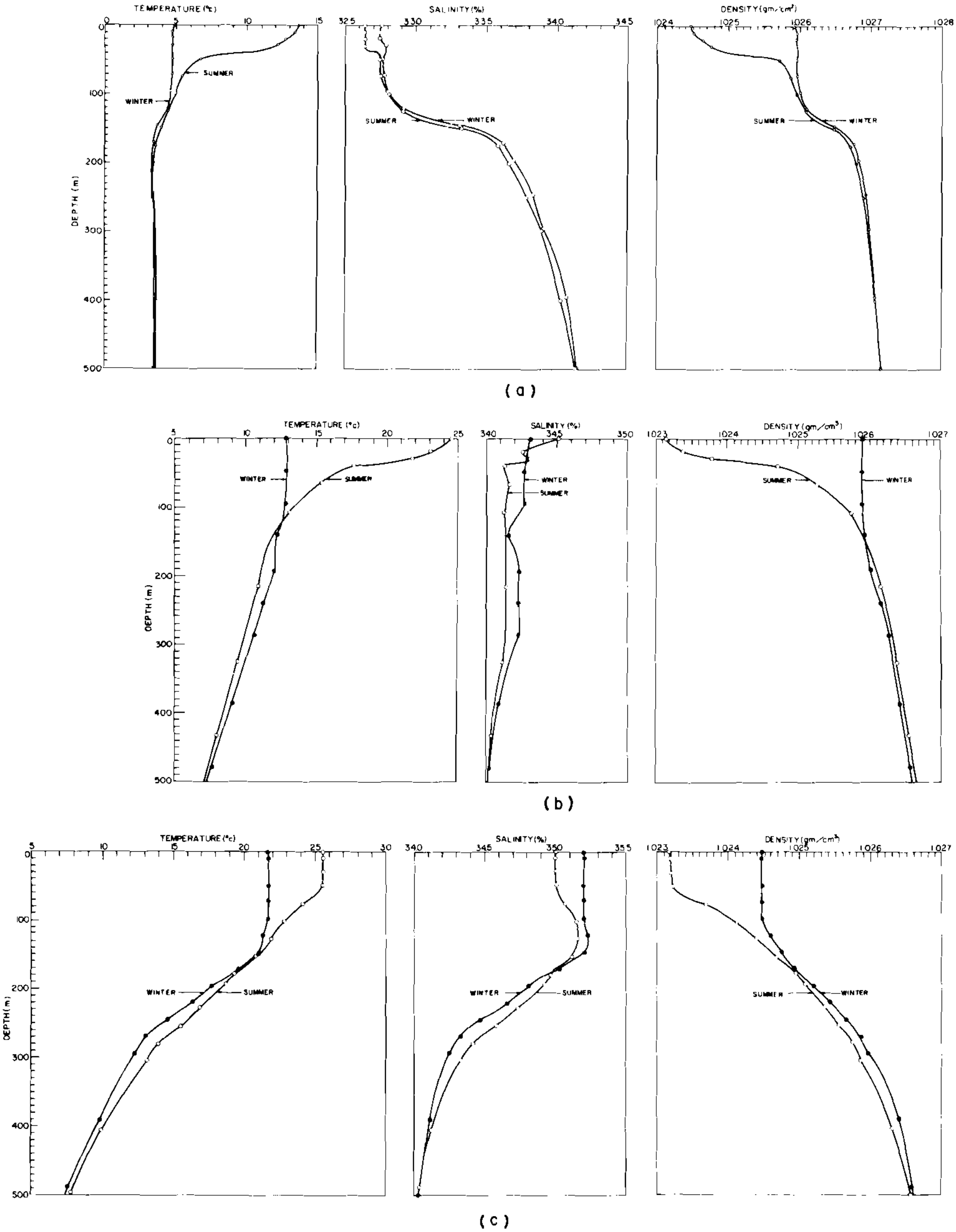

Fig. 16 Salinity (‰), temperature (°C) and density (g/cm³) of upper 500 metres of water column in the North Pacific Ocean. (a) Subarctic Region: Station *P* (50°N, 145°W); 9 September 1964, 26 February 1965 (Canadian Oceanographic Data Centre, 1965; 1966). (b) Subtropical Region: Station 60 (35° 28′N, 159° 33′W, 17 February 1955). Station 100 (35° 56′N, 157° 30′W, 24 August 1955) Scripps Inst. Oceanogr. of the Univ. of California, 1962. (c) Subtropical Region: Station 40 (25° 00′N, 157° 00′W, 19 September 1964, 26 February 1965) Charnell *et al.*, 1967a, 1967b.

upper 30 m although it is more common to observe an upper isothermal layer of thickness 20–50 m. In the depth range between 100 and 500 m, the temperature changes little with depth and frequently one or more inversions are present. The temperature then decreases gradually to 3 to 4°C at 500 m and to 1.5°C at the ocean floor. In the Subarctic region, however, it is the salinity, not the temperature, which determines the vertical density structure and therefore determines the stability of the water column – at least in the upper 500 m.

It should be noted that, because of the presence of the marked halocline, the winter convective overturn is unable to mix the water deeper than the halocline. Hence, it is possible that the upper layer of the ocean will continue to cool if heat loss from the sea surface is occurring. Only through erosion of the halocline by intense evaporation at the surface can such an effect be altered.

In the Subtropic region, evaporation exceeds precipitation so that no marked halocline is formed. In fact, the salinity generally decreases gradually to a minimum at a depth varying between 200–600 m, below which it gradually increases. An example of the water structure here is represented by the data shown in Fig. 16b taken approximately 1600 km south of Station P. The temperature structure of the upper 100 m depth is similar to that encountered in the Subarctic region: that is, it is isothermal in winter but has a marked thermocline between depth 30 m and 50 m in summer. Another similarity is that the upper 30 to 50 m is usually isothermal though this is not indicated in this particular figure. There are differences, however. For one thing, the thermocline, though less intense than its Subarctic counterpart, continues to a greater depth. In addition, because of the lack of a definite salinity gradient in the halocline, and because the salinity decreases with depth rather than increases as it does in the Subarctic region, the thermal structure of the water here is necessarily determining the stability of the water column. It must then also determine the extent to which convective mixing can penetrate. Further to the south – approximately 1100 km to the south of the previous location (north of the Hawaiian Islands) but still in the Subtropic region – the salinity can take on another feature as shown in Fig. 16c. Here the salinity can increase with depth between the depth of 50 m and 130 m from where it decreases with depth, as was the case for the previous location. Another difference between the salinity structure of these latter two locations is that the rate of salinity decrease in layers between the depth of 150 m and 300 m is considerably greater in the more southern location. Also, the thermal structures are different. In the more southern area, the summer thermocline in the upper 100 m joins the other permanent thermocline and appears as one broad thermocline. The density structure here is again determined by the thermal structure at a depth greater than 100 m but in the upper layer the small halocline present can be effective in controlling convective mixing. However, this halocline is not large enough to impede vertical mixing and once broken by excess evaporation over precipitation, the extent of the convective overturn would then be governed by the thermal structure. (The above three examples were taken from data taken along the meridian between longitude 145°W and 160°W. In a section either west or east of this, slight differences from the structures can be expected, but the essential characteristics as shown here for the two main regions are considered representative.)

The Subarctic region is also characterized by a net annual heat loss, particularly off the coast of Japan, where the Kuroshio waters become exposed to colder, drier air, especially in the winter. The average long-term annual heat loss off Japan has been estimated to be as high as 200 g-cal cm^{-2}/day, but further east at the longitude of the International Date Line and along the Aleutian Islands there is no net annual loss (Wyrtki, 1965). At Station P an annual gain of about 66 g-cal cm^{-2}/day has been estimated (Tabata, 1965). Except off the east coast of Japan the region receives more fresh water by precipitation than loss by evaporation (Jacobs, 1951).

In the Subtropic region there is generally a net annual heat gain by the ocean except in an area east of the Hawaiian Islands and off the west coast of Colombia to the north of the Equator. This region is also featured by net water loss due to excess evaporation over precipitation, except to the north of the Equator where appreciable excess precipitation over evaporation occurs (Jacobs, 1951).

As already stated, the convective overturning in both the Subarctic and Subtropic regions can extend to a depth of 100 m or more. Since within these limits the extent of the overturn is governed by the seasonal changes of the forcing functions – the forced convective mixing due to wind and wave stirring and free convective mixing due to the excess evaporation over precipitation and heat loss – it will be useful to examine the seasonal changes of the thermal structures and see if there are similarities or contrasts between the two main regions.

To illustrate these, the monthly changes in thermal structure at the three ocean stations will be considered: Station P (50°N, 145°W), Station V (34°N, 164°E), (⅔ of the way between the Hawaiian Islands and Japan); and Station N (30°N, 140°W), (half way between San Francisco and the Hawaiian Islands). Station P, as you may recall, is in the Subarctic region where there is an average annual heat gain of 66 g-cal cm^{-2}/day and excess precipitation over evaporation of 25 cm/year. Station V, located in the Subtropic region close to the Subarctic Boundary, is in an area where there is an annual heat gain of 50 g-cal cm^{-2}/day (Wyrtki, 1965) and an annual loss of water by excess evaporation over precipitation of 80 cm/year (Jacobs, 1951). Station N, also in the Subtropic region, lies west of the path of the California Current. It is in an area where there is no significant annual heat gain and where the annual water loss due to excess evaporation over precipitation has been estimated by Jacobs to be also 80 cm. Recent estimates of precipitation at Station N (Dorman *et al.*, 1974), however, have yielded a value that is only one-half of what Jacobs has suggested. If true, revision of the annual water loss would be nearer to 100 cm than 80 cm.

A comparison of the monthly changes in thermal structure at the three locations (see Fig. 17) shows that, despite the difference in their locations, the seasonal changes of the thermal structures are similar, except that the annual range of temperature at Station N is the smallest and at Station V the largest.

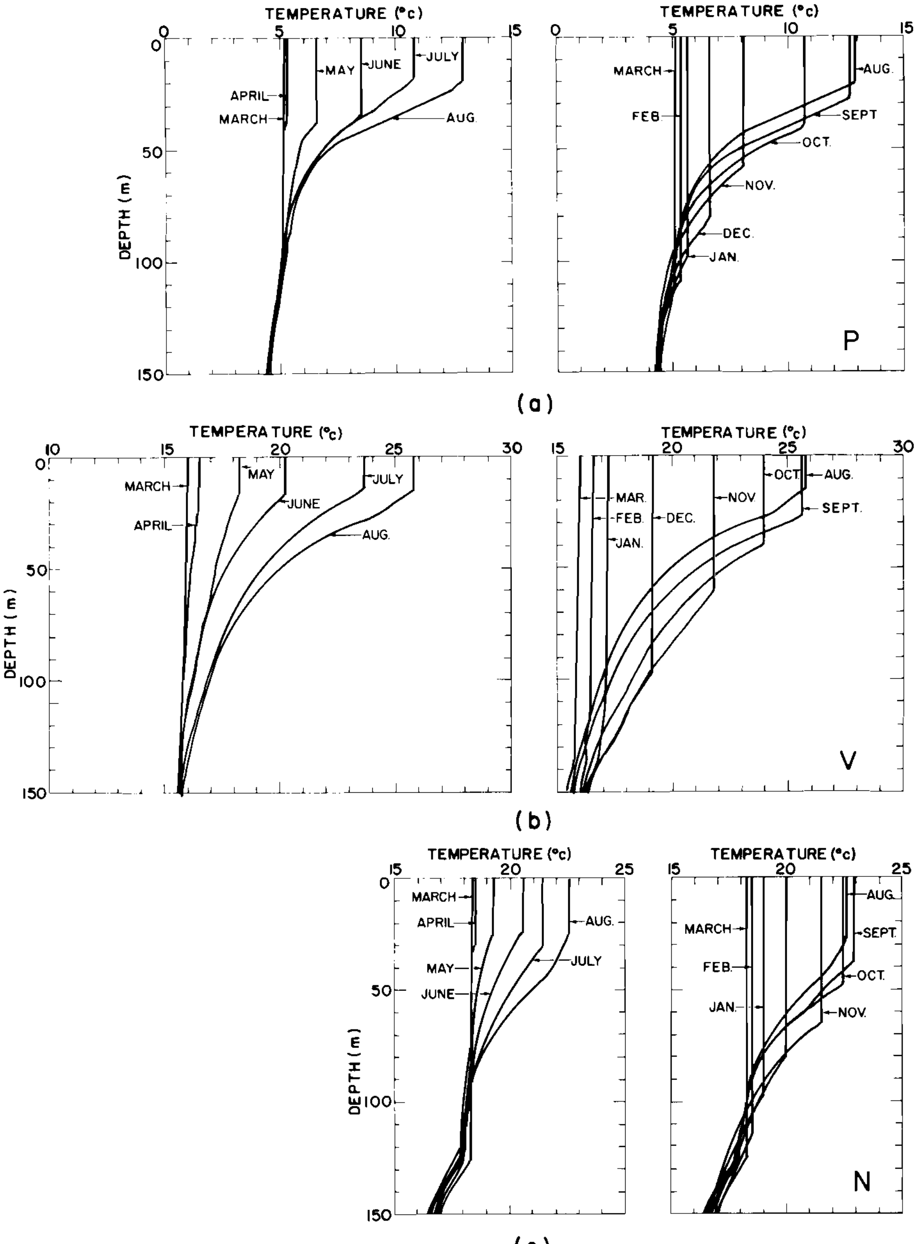

Fig. 17 Monthly mean thermal structures at the three Ocean Weather Stations (°C). (a) Station P (50°N, 145°W) (Based on 19-year means – 1950–1968) (Ballis, 1973a) (b) Station V (34°N, 164°E) (Based on 16-year means – 1955–1970) (Ballis, 1973b) (c) Station N (30°N, 140°W) (Based on 24-year means – 1947–1971) (Ballis, 1973c).

At the three Stations the minimum temperature is reached in March and the maximum in August or September. But the heat content is at a maximum in September in all cases. In many other areas the surface temperature reaches a maximum in August, but it is likely in these areas that because the heat is distributed to greater depth, the heat content is at a maximum in September despite the lower surface temperatures. There is some evidence that the extent of the convective overturn, as inferred from the structures in March, is tens of metres greater at Stations N and V than at Station P.

Detailed time sequences of the salinity structure are only available for Station P. They show that, during the summer months, the salinity in the upper 30 m or so decreases and can be completely accounted for by consideration of the gain of fresh water by excess precipitation over evaporation (Tabata, 1965). The salinity generally increases from September to March and this is mainly due to the convective overturn which mixes the less saline water of the upper layers with the more saline water lying below.

It has been shown, at least for the summer months in the Subarctic region, that the upper mixed layer is produced by wind mixing, the depth of the mixed layer being primarily a function of wind speed (Tabata *et al.*, 1965). Even as close as 300 km to the coast of Washington state, this relationship holds (Halpern, 1974). During the cooling season between September through March the effect of free convection superimposed on that of forced convection is evident (Tabata, 1965). A variety of models proposed recently (Denman, 1973; Denman and Miyake, 1973; Pollard *et al.*, 1973) seem capable of predicting the deepening of the mixed layer depth in summer due to forced convection but a satisfactory model incorporating the effect of free convection has not yet been formulated.

While the heat content of the upper 100 m or so of the water column is determined mainly by the heat flux across the atmosphere-ocean boundary, it is the effect of convective mixing that permits the thermal structures to assume their characteristic features. Similarly, the fresh water flux at the air-sea boundary determines the salt content of the upper layers but again it is the convective mixing that gives the salinity structure its characteristic features.

The horizontal transport of water can also affect the thermal structure. However, it is unlikely to affect the main thermal structure unless a different water mass intrudes into the area, as often occurs in the region of the Kuroshio-Oyashio convergence zone. Generally speaking, the vertical transport resulting from the horizontal divergence or convergence of the wind-driven transport probably can alter the structures to a larger extent than can the horizontal transports. Along the coast and at the Equator, the Ekman transport can be effective in drawing water from the greater depths and altering the structure. In the open ocean and away from the Equator, the curl of the wind stress can be effective in raising or lowering the depth of the thermocline (Yoshida, 1967b; Robinson, 1968). But these effects are not likely to be readily observable in a time scale of days, except in the presence of violent storms; nevertheless, they might be detectable over periods of months.

It has been shown at Station P that in order to maintain the observed salinity and temperature structures it is necessary to bring in colder, more saline water to the upper layers. Slow upwelling of water at speeds of the order of 10 to 20 m/year would be sufficient to maintain the salinity structure but would only account for 10–20% of the surplus heat. Much of the surplus heat at Station P can be removed by the influx of cold water from a region west to northwest of Station P (Tabata, 1965). One could assume that under steady-state conditions, the slow diffusion of heat and fresh water downward can be balanced by this steady, slow upwelling. In other areas of the Subarctic region having similar climates, similar processes should prevail.

Because the halocline prevents vertical mixing from penetrating beyond 150 m, the redistribution of heat in the upper mixed layer should not vary greatly in the Subarctic region from year to year. However, in the Subtropic region this restriction is removed and given sufficient cooling and evaporation during the autumn and winter, mixing may reach depths much beyond those shown in the examples. Should such changes in the convective overturn occur, the temperature of the upper mixed layer would decrease further, not only from heat loss at the surface, but because of the colder water being upwelled from below into the upper layer. However, by so doing, the warmer water of the upper layers are now mixed into the lower layer, so that the lower layers will experience an increase in temperature, thus storing heat for possible future use. It follows that the intensity of convective overturn, especially in the Subtropic and likely also in the Tropic regions, will have important bearings on the temperature of the upper layers of the ocean, and one should consider it when attempting to account for temperature anomalies.

11 Influence of the ocean on the climate

I am somewhat hesitant to discuss the influence of the ocean on climate because at the moment I am not too certain what this influence really is. However, in order that my presentation have some relevance to our theme topic, I shall mention the few examples I have come across.

The relatively cool summers and the warm winters we experience along the Pacific coast of the northwestern United States and British Columbia are attributable, respectively, to the presence of cold water along the coast due to upwelling and to the presence of relatively warm water in the North-east Pacific off our coast. The cool climate along the Peru-Chile coast is associated with the cooling effect caused by upwelling and by the influx of cold water from the Antarctic region. These examples are familiar to practically all of us. The occurrence of a poor rice crop in northern Japan is apparently due to the presence of cooler weather associated with the intrusion of the cold Oyashio water from the north during periods of northerly winds. This effect is so well known in Japan that in the country there is a saying that "the poor harvest comes from the sea".

However, it was not until 1959, when Namias (1959) first suggested there may be a close interaction between the atmosphere and the ocean and that the ocean climate might affect the mean general atmospheric circulation over the North Pacific Ocean, that intense interest in the large-scale air-sea interactions really took root. He drew attention to the possible large-scale influence of the Pacific Ocean on the climate of continental North America and concluded in his study that anomalously high sea-surface temperatures were the result of anomalous atmospheric circulation patterns over the Pacific Ocean and that high ocean temperatures in turn, strongly influenced the overlying atmospheric circulation.

Bjerknes (1966a, 1966b) pursued this problem of large-scale air-sea interaction and was the first to suggest that the Pacific Ocean temperature anomalies may have even a greater impact on the circulation of the northern hemisphere, or for that matter on the globe. In his studies related to the warming of water along the Pacific coast of South America in 1957–1958, he suggested the following sequence of events that led from one locality to larger areas:

1. Southeast Trades weaken along the eastern side of the Equatorial Pacific;
2. Upwelling along the Equator ceases, which then
3. Leads to warming of the upper layers of the eastern Equatorial Pacific;
4. This then leads to the warming of the overlying atmosphere;
5. Convection over the Equator intensifies, which results in
6. Increased precipitation;
7. The warmer than normal equatorial area results in the acceleration of the Hadley circulation and to the transport of absolute angular momentum to the subtropical jet stream at a faster rate than normal.
8. The continued poleward flux of absolute angular momentum and its downward flux in the belt of the surface westerlies results in an intensification of the westerlies in the North Pacific;
9. The Subtropical High is then shifted to the south and with the strong westerlies developed, the Aleutian Low intensified during the winter of 1957–58;
10. This then leads to a large-scale downwind effect carried by the upper westerlies, which then
11. Leads to the weakening of the Icelandic Low and sets the stage for a cold winter in northern Europe.

However, Doberitz *et al.* (1967) have cast some doubt regarding some of Bjerknes' interpretations. More recently, Ramage (1970) has suggested that the sequence of events also leads to the extension eastward (from the east of the dateline) of the near-equatorial trough in both hemispheres. Moreover, he suggests that the development of depressions in the troughs, which successively develop farther eastward, results in a reversal of the normal direction of the pressure gradient along the Equator. The westerlies that then develop progressively from the west, being convergent, result in the rising of air and the heavy rainfall associated with it.

A course of events similar to those for the winter of 1957–58 was repeated in 1963–64 and 1965–66 in the equatorial Pacific (Bjerknes, 1969). In a more recent study, Bjerknes (1972) further strengthened the validity of his hypothesis by noting that the subtropical westerly jet was stronger in 1965 compared to 1964 and that the Aleutian Low had been displaced westward from 1964 to 1965. He further pointed out that the circulation in the mid-latitudes can also be affected by the heat transported by the Kuroshio.

The importance of upwelling in the equatorial Pacific to the atmosphere has been given further emphasis by Flohn (1972) who demonstrated its attendant influence on cloudiness and rainfall in the area.

Namias (1962, 1963, 1969a, 1969b) has subsequently produced a variety of studies related to the large-scale atmosphere-ocean interaction. In one study, Namias (1969a) asserts that the large changes in the monthly mean atmospheric circulation over the Pacific and Atlantic Oceans, which frequently occur in the autumn are partly due to the influence of extensive areas of unusually warm or cold waters generated during the antecedent summer. In another study, Namias (1966) related the occurrence of droughts in the northern United States during 1962–65 to the effect of large-scale air-sea interaction over the Pacific Ocean at that time.

In such phenomenological air-sea interactions in which an oceanic event may lead to an atmospheric event or vice-versa, it is difficult to conclude which event was initially responsible for the chain of events that followed. Dubin (1973), for example, found a close relationship between the North Pacific sea surface temperature anomalies during the 1960's and hail damage in Alberta. But he was unable to ascertain whether the marked reduction in hail damage for the summers of 1962 through 1967, associated with the southward shift of the jet stream maximum, was due to the sea surface temperature anomalies or whether the mechanism responsible for the anomalies caused the reduction in the hail damage.

The meridional atmospheric teleconnections over the North Pacific during the period from 1950 to 1972 have recently been examined by White and Walker (1973) who found that large-amplitude year-to-year variations in the strength of the Aleutian Low during 1950–63 were generated independently of the convective activity at the Equator. On the other hand, the small-amplitude year-to-year fluctuations during 1964 to 1972 were closely connected. Thus, the large-scale relationship between the events in the Equator and the higher latitudes are still not as clear as some investigators have proposed.

While much of the large-scale air-sea interaction studies have been centred on a large area of the North Pacific, Japanese investigators have considered the oceanographic conditions in the Bering Sea to be of primary importance for climatic changes in Japan – so much so that in the past they had conducted oceanographic surveys in these northern waters and on the basis of the results predicted the yield of the Japanese rice crop (M. Hanzawa, personal communication). The importance of the Bering Sea to the climate in Japan in late spring is apparently related to the presence of cold water there which results in the formation of a trough in the troposphere over the Bering Sea. This in turn stimulates the formation of a low-level anticyclone (Okhotsk High) which then advects colder air over Japan (Okawa, 1974). Furthermore, the accompanying increase in the northerly winds would likely strengthen the Oyashio, thereby augmenting the cooling of the water and the overlying atmosphere in the vicinity of Japan.

Another example of the possible influence of the ocean on climatic change has been proposed by Weyl (1968). In his hypothesis, Weyl emphasizes the importance of oceanic salinity. He argues that changes in the surface salinity distribution of the world ocean can, by changing the extent of sea ice in the North Atlantic and Antarctic Ocean, lead to climatic changes – including a drastic change such as the coming of an ice age. His arguments are as follows:

If the North Atlantic Ocean were to have a surface salinity as low as the Pacific Ocean, a large part of the North Atlantic Ocean would be covered by ice due to the effect of salinity on the freezing point of sea water. Because the sea ice alters the heat balance of the atmosphere, firstly because of the increased albedo of the sea surface covered by ice and secondly because the presence of sea ice impedes the transfer of heat between the atmosphere and the ocean, there will then be a reduction in warming in the polar seas. This will then lead to the cooling of a large area of the Northern European Continent because of southward shift of the Icelandic Low.

A reduction in the salinity of the Atlantic Ocean could be accomplished if it were possible to reduce the westward transport of water vapour across the Isthmus of Panama from the Atlantic. At present, this water vapour precipitates and falls on the eastern side of the Pacific. Weyl (*ibid.*) quotes Deffeys (personal communication) who claims that the water vapour transport is equivalent to a transport of fresh water from the Atlantic to the Pacific amounting to 1/10 of a sverdrup – equal to 10% of the discharge of all the rivers of the world! So, if the vapour transport were reduced drastically by some atmospheric anomaly, the Atlantic would have a lower salinity and therefore a more extensive ice cover would ensue. Weyl further showed that the events leading to the "Little Ice Age" tend to confirm his hypothesis.

We have quoted some examples of the possible effects of the ocean on the climate. Most of the studies are conceptual in nature and, although some evidence has been provided to back the hypotheses, none have been adequately tested. A recent numerical study by Rowntree (1972), using the 9-level hemispheric model of atmospheric circulation developed at the Geophysical Fluid Dynamics Laboratory (in Princeton, U.S.A.), has been used to test Bjerknes' hypothesis that the variations of the sea surface temperatures in the eastern part of the Equatorial Pacific are responsible for the variations and intensity of the Aleutian Low. The numerical results indeed showed that, given a maximum anomaly of 3.5°C for the sea surface temperature, the hypothesis can be confirmed. However, the model utilizes a "wall" at the Equator and such a "wall" can distort the wind and temperature field in the higher latitudes (Miyakoda and Umscheid, 1973). For this reason, Ramage and Murakami (1973) argue that the test is not complete. Despite the deficiencies in the model, it is a first attempt to show numerically that the sea surface anomalies can cause a change in the general circulation. The hypotheses of Bjerknes and Namias should be further tested by a more complete model.

Of course, part of the difficulty in relating the oceanic events to those of the atmosphere can be attributed to the different response time of the ocean from that of the atmosphere. In the numerical experiments of the atmosphere-ocean coupled model, the atmospheric circulation would stabilize in about a month while the ocean would not stabilize fully even when the model was run for the equivalent of two hundred years. The other difficulty is the cost of initial capital investment in procuring a large computer system and the expense to run it. However, such a study is essential, as large-scale climatic changes can have drastic economic consequences and our ability to predict these changes certainly should help mankind.

12 Summary and conclusions (parts I and II)

Our knowledge of the distributions of surface currents and sea surface temperature is more complete than that of other quantities, principally because of the greater amount of data. These data are mainly based on information collected by merchant and naval vessels of the world's maritime nations. However, because the merchant ships ply well established routes there are obvious gaps in the data they collect. Nevertheless, this information has been of enormous help to oceanographers, despite the fact it is not always accurate. Improvement upon the quality of the data gathered would be of immense value.

The mean velocities of the major current systems are all we have at the moment, except for a few currents such as the Kuroshio and some of the equatorial currents about which we have some vague ideas concerning their seasonal fluctuations. At present, the only area where surface currents are being observed regularly is within 500 km of the Pacific coast of Japan.

There has been only one comprehensive study made of the water movement in the intermediate layers of the Pacific Ocean. Yet, the motion in these layers is likely to have profound effects upon the water mass transport and heat transport. It is of particular importance that the latter be determined correctly if we are to resolve the problem of the direction of heat transport so vital to the consideration of the heat exchange between the atmosphere and the ocean. Where the currents of the deep bottom-water have been estimated, there is a general consistency amongst the results; however, the oceanic areas covered by the data is so limited that a complete picture of the deep water circulation is still unavailable. Although the volume transport has been estimated for many of the major currents, assumptions used to obtain the integrated transport above an arbitrary "level of no-motion" are by no means consistent. Further, some transports are based on the geostrophic transports and have had to be modified to accommodate the current speeds measured at large depths. Others are based solely on measured current velocity values. This makes it difficult to make a meaningful comparison between the various transport values.

There has been only a limited number of studies conducted on heat transport in the Pacific Ocean. Some of the results are even in conflict as to the general direction of transport, whether it is toward the Equator or toward the pole. Those who have proposed an equatorward flow in the upper layers of the ocean have invoked a circulation in the meridional plane involving ascending movement of water which is, at the present time, little known or understood. If circulation in the vertical plane is to be considered, it is almost certain that, in addition to the wind-driven circulation that we have been emphasizing, we must also consider the thermohaline circulation resulting from differential heating and cooling, from differences in evaporation and precipitation and from the freezing and melting of sea ice.

Another problem associated with the estimate of oceanic heat transport is the limited accuracy of heat flux computations. An error of more than 10% is to be expected in the estimates of radiational flux and even more in the turbulent flux. Such errors are liable to affect the calculation of heat gain or loss, as the heat surplus calculated for the North Pacific is only about 10% of the incoming solar radiation alone.

Thus, the two items, the determination of circulation in the meridional plane and the upgrading of heat flux estimates, deserve careful study.

A variety of numerical models of ocean circulation have been produced to examine the ocean currents. Most of these models reproduce results that agree with the observations in some regions but not in others. At the moment the model results are not much better than those obtained from the application of the classical wind-driven circulation theories. One of the more important findings of the coupled ocean-atmosphere circulation is the long response-time indicated for the ocean compared to that for the atmosphere. While the modelled atmospheric circulation resembled the observed circulation in a matter of months, the ocean circulation did not stabilize even after the model had been run for a few hundred years.

The main features of the distribution of sea surface temperature have been described and it was pointed out that the deviations of the isotherms from a zonal orientation were due to advective and convective effects.

The discussion of the thermal and salinity structures is based on a few examples from the Subarctic and Subtropic regions. It was shown that the seasonal changes in the oceanic thermal structures are similar in the upper 100 m or so. It is pointed out that in the Subarctic region at least, the thermal structures are governed by the heat flux across the air-sea boundary and by the degree of convective mixing, and less so by horizontal water transport. Further, while the salinity structure in the Subarctic region determines the depth to which the winter convective overturn can penetrate, in the Subtropic region it is the thermal structure that plays a leading role in determining the depth to which overturn could penetrate. In addition to the above, vertical transport of water resulting from the divergence of the Ekman transport might have some influence in determining the heat content in the upper layers of the ocean. The Subarctic region is a divergent zone, and therefore upwelling of water can reduce the amount of heat in upper layers. Near the coast, the Ekman transport away from the coast can accomplish the same thing, but in the open water the vertical transport is related to the curl of the wind stress. Near the Equator, the Ekman transport away from the Equator can also result in cooling.

The most conspicuous seasonal changes in wind velocity appear to occur in the western side of the Equatorial Pacific. However, there seems to be only a few comprehensive studies to clarify the possible changes of currents that result from the reversal of winds there. From studies conducted along the Eastern Equatorial Pacific, changes in the general location of the wind field, such as changes in the position of the Intertropical Convergence Zone, rather than the intensity of winds, appear to be of greater importance to the distribution of ocean circulation in that region.

Although sea surface temperature anomalies over relatively large areas are present in various locations in the North Pacific Ocean, the largest anomalies occur in the equatorial region where it is not uncommon to observe an anomaly of $\pm 4°C$.

Large-scale phenomenological air-sea interaction studies conducted in the past, focussed their attention on the equatorial anomalies. Although these studies are in their early stages of development and therefore have deficiencies, at least one numerical study has indicated that the hypotheses proposed on this subject may have some substance. No doubt many of the hypotheses deserve testing by various methods, amongst which numerical modelling may be most promising.

From the standpoint of the possible influence of ocean currents upon the climate there are certain regions that require attention. The termini of the various equatorial currents seem to be some of the most important regions as the events there would determine the amount of heat that would be available for poleward transport. The degree to which the Peru Current affects the temperature of the lower latitudes of the eastern South Pacific Ocean will depend upon how much of the eastward-flowing South Pacific and Antarctic Circumpolar Currents is diverted poleward. The Kuroshio is a source of heat in the North Pacific Ocean but its dominant influence may be considerably modified by the southward-flowing cold Oyashio. Because of the importance of the Bering Sea in influencing the climate of Japan and its possible influence on the overall North American climate as a consequence of variations in its ice cover, the amount of warm Pacific water entering the sea should be important to climatological studies.

In closing, I wish to state that this present review is far from complete. I have attempted to update the present status of our oceanographic knowledge as much as possible, but in my haste to include some of the recent developments I have probably omitted other pertinent information which should have been considered. I have deliberately made little reference to the many important studies of the Atlantic Ocean as its inclusion would have made this review much too long. I do not believe that I am understating the case if I say that our knowledge of the ocean circulation is still in the early stage of development. In fact, it was only over two and one-half decades ago that the large Equatorial Under-current was discovered. The South Equatorial Countercurrent was discovered within the last two decades, and, although not all the oceanographers agree to its existence, there is sufficient data to indicate that some type of eastward flow is present. In the eastern Subtropic region, the possibility of there being a Subtropical Countercurrent has been suggested, and, although there is a body of evidence indicating its occurrence, more data are needed to confirm its existence. There are probably other appreciable currents that we are not yet aware of. Also our knowledge and the understanding of the meridional circulation in the vertical plane is still very poor and the thermohaline aspect of the circulation is still ignored in most numerical models. All of these need to be studied by our collective effort if we are to apply our oceanographic knowledge to the consideration of the ocean's impact on the climate.

Acknowledgement

When preparing a review paper such as this, with only a few months notice, it is not easy to do without the able assistance of many individuals. I wish to acknowledge those who have been most helpful: our computing service and clerical staff, librarian, photographer and especially Patricia Kimber for preparing the illustrations. I am grateful to Mr. Andrew Bakun of the National Marine Fisheries Service, NOAA, for providing me with updated sea-level atmospheric pressure data for the North Pacific obtained from the U.S. Navy Fleet Numerical Weather Central, to Mr. Joseph Reid of the Scripps Institution of Oceanography and to Dr. John Knauss of the University of Rhode Island for permitting me to use illustrations published elsewhere; I am particularly grateful to Mr. Joseph Reid and Dr. Robert Arthur of the Scripps Institution of Oceanography for providing me with an unpublished illustration depicting winter geostrophic circulation of the Pacific Ocean. I appreciate the assistance of Dr. R.E. Thomson, who provided critical and helpful comments, and lastly I am grateful to the Canadian Meteorological Society for giving me an opportunity to acquaint our meteorologists with the oceanography of the Pacific Ocean.

References

ALBRECHT, F., 1960: Jahreskarten des Wärme- und Wasserhaushaltes der Ozeane. *Ber. Deut. Wetterdienstes*, **66**, Bd. 9, 19 pp. (Quoted by Bryan, 1962).

BALLIS, DOUGLAS H., 1973a: Monthly mean bathythermograph data from Ocean Weather Station "PAPA". SIO Reference Series, 73–5, Scripps Institution of Oceanography, 101 pp.

———, 1973b: Monthly mean bathythermograph data for Ocean Weather Station "VICTOR". SIO Reference Series, 73–6, Scripps Institution of Oceanography, 82 pp.

———, 1973c: Monthly mean bathythermograph data from Ocean Weather Station "NOVEMBER". SIO Reference Series, 73–3, Scripps Institution of Oceanography, 121 pp.

BJERKNES, JACOB, 1966a: Survey of El Nino 1957–58 in its relation to tropical Pacific meteorology. *Inter-American Tropical Tuna Commission*, Bull. **12**, No. 2, 62 pp.

———, 1966b: A possible response of the atmospheric Hadley circulation to equatorial anomalies of ocean temperature. *Tellus*, **18**, 820–828.

———, 1969: Atmospheric teleconnections from the equatorial Pacific. *Monthly Weather Rev.*, **97**, 163–172.

BRYAN, K., 1962: Measurements of meridional heat transport by ocean currents. *J. Geophy. Res.* **67**, 3403–3414.

———, 1969: The Ocean Model. *Monthly Weather Review*, **97**, 806–827.

———, S. MANABE and RONALD C. PACONOWSKI, 1975: A global ocean atmosphere climate model. Part II. The Ocean Circulation. *J. Phys. Oceanogr.* **5**, 30–46.

BUDYKO, M.I., 1956: The Heat Balance of the Earth's Surface (Translated by N.A. Stepanova, 1958), U.S. Dept. of Commerce, Wash., D.C., 259 pp.

CALIFORNIA DEPARTMENT OF FISH AND GAME, MARINE RESEARCH COMMITTEE, 1960. *The Changing Pacific Ocean in 1957 and 1958.* Editors: Oscar Sette and John D. Isaacs. California Cooperative Oceanic Fisheries Investigations Reports, Vol. VII, 217 pp: 205–217.

CANADIAN OCEANOGRAPHIC DATA CENTRE, 1965: Ocean Weather Station P, North Pacific Ocean, August 7 to October 31, 1964. 1965 Data Record Series, No. 7. 118 pp.

———, 1966: Ocean Weather Station P, North Pacific Ocean, January 23, 1965 to April 19, 1965. 1966 Data Record Series, No. 1, 122 pp.

CHARNELL, ROBERT L., DAVID W.K. AU and GUNTER R. SECKEL, 1967a: The Trade Wind Zone oceanography pilot study Part II: *Townsend Cromwell.* Cruise 4, 5, 6. May to July 1964. Special Scientific Report – Fisheries 553, U.S. Dept. of the Interior, Fish and Wildlife Service, Bur. of Commercial Fisheries, 78 pp.

———, 1967b: The Trade Wind Zone oceanography pilot study Part IV: *Townsend Cromwell.* Cruise 11, 12 and 13. December 1964 to February 1965. Special Scientific Report – Fisheries 555, U.S. Dept. of the Interior, Fish and Wildlife Service, Bur. of Commercial Fisheries, 78 pp.

CLOWES, A.J., 1933: Influence of the Pacific on the circulation in the southwest Atlantic Ocean. *Nature*, **131**, 189–191.

DEFANT, ALBERT, 1961: *Physical Oceanography*, Vol. 1. Pergamon Press, New York, Oxford, London, Paris, 729 pp.

DENMAN, K.L., 1973: A time-dependent model of the upper ocean. *J. Phys. Oceanogr.*, **3**, 173–184.

——— and M. MIYAKE, 1973: Upper layer modification at Ocean Station Papa: Observations and simulation. *J. Phys. Oceanogr.*, **3**, 185–196.

DOBERITZ, R., H. FLOHN and K. SCHÜTTE, 1967: Statistical investigations of the climatic anomalies of the equatorial Pacific. *Meteorol. Abhand.* **7**, 76 pp.

DORMAN, CLIVE E., C.A. PAULSON and W.H. QUINN, 1974: An analysis of 20 years of meteorological and oceanographic data from Ocean Station N. *J. Phys. Oceanogr.*, **4**, 645–653.

DUBLIN, JOHN, 1973: The relation between the North Pacific sea surface temperature anomaly during the sixties and hail damages in Alberta. *Atmosphere*, **11**, 41–51.

EBER, L. and F. MILLER, 1974: Sea surface temperature and environmental conditons. Fishing Information, August 1974, No. 8, U.S. Dept. of Commerce, Nat. Oceanic and Atmospheric Administration, National Marine Service, 16 pp.

FAVORITE, FELIX and DOUGLAS R. MCCLAIN, 1973: Coherence in Transpacific movement of positive and negative anomalies of sea surface temperature, 1953–60. *Nature*, **244**, 139–143.

FLOHN, H., 1972: Investigations of Equatorial upwelling and its climatic role. In *Studies in Physical Oceanogr.* (A.L. Gordon, editor) Gordon & Breach, Science Publishers, New York and London, Vol. 1, 194 pp, 93–102.

GILL, A.E. and P.O. NIILER, 1973: The theory of the seasonal variability in the ocean. *Deep Sea Res.*, **20**, 141–177.

HALPERN, DAVID, 1974: Observations of the deepening of the wind-mixed layer in the Northeast Pacific Ocean. *J. Phys. Oceanogr.*, **4**, 454–466.

HOUGHTON, H., 1954: On the annual heat balance of the northern hemisphere. *J. Meteorol.*, **11**, 1–9.

JACOBS, WOODROW C., 1951: The energy exchange between sea and atmosphere

and some of its consequences. *Bull. Scripps Inst. of Oceanography*, **6**, 27–122.
LAVIOLETTE, PAUL E. and SANDRA E. SEIM, 1969: Monthly charts of mean, minimum and maximum sea surface temperature of the North Pacific Ocean. Special Publ. SP-123, Naval Oceanogr. Office, Wash. D.C., 57 pp.
MANABE, SYUKURO, 1969: The atmospheric circulation and the effect of heat transfer by ocean currents. *Monthly Weather Rev.*, **97**, 775–805.
———, KIRK BRYAN and MICHAEL J. SPELMAN, 1975: A global ocean-atmosphere climate model. Part I. The atmospheric circulation. *J. Phys. Oceanogr.*, **5**, 3–29.
MARITIME SAFETY AGENCY, 1971: Current Charts in the Adjacent Seas of Nippon. 2nd Series, 1955–64, No. 6041, Tokyo. 40 plates.
MASUZAWA, JOTARO, 1972: Water characteristics of the North Pacific central region. *Kuroshio, its physical aspects* (H. Stommel and K. Yoshida, editors), Univ. Tokyo Press., 517 pp, 95–127.
MIYAKODA, K. and L. UMSCHEID, JR., 1973: Effects of an equatorial "wall" on an atmospheric model. *Monthly Weather Review*, **101**, 603–616.
MORIYASU, SHIGEO, 1972: The Tsushima Current. *Kuroshio, its physical aspects* (Henry Stommel and Kozo Yoshida, editors). Univ. Tokyo Press, 517 pp, 353–369.
NAMIAS, J., 1959: Recent seasonal interactions between North Pacific waters and the overlying atmospheric circulation. *J. Geophys. Res.*, **64**, 631–646.
———, 1962: Influences of abnormal surface heat sources and sinks on atmospheric behaviour. Proc. of the International Symposium on Numerical Weather Prediction, Meteorol. Soc. Japan, Tokyo, 615–627.
———, 1963: Large-scale air-sea interactions over the North Pacific from summer 1962 through the subsequent winter. *J. Geophys. Res.*, **68**, 6171–6186.
———, 1965: Macroscopic association between North Pacific Waters and overlying atmospheric circulation. *J. Geophys. Res.*, **68**, 2307–2318.
———, 1969a: Autumnal variations in the North Pacific and North Atlantic anticyclones as manifestation of air-sea interaction. *Deep Sea Res.*, Supplement to Vol. **16**, 153–164.
———, 1969b: Seasonal interactions between the North Pacific Ocean and the atmosphere during the 1960's. *Monthly Weather Review*, **97**, 173–192.
OHTANI, K., 1970: Relative transport in the Alaskan Stream in winter. *J. Oceanogr. Soc. Japan*, **26**, 271–282.
OKAWA, T., 1974: Intensification of the Okhotsk High due to cold sea surface. Oceanography of the Bering Sea with emphasis on renewable resources (D.W. Hood and E.J. Kelly, editors), Occasional Publ. No. 2 Inst. of Marine Science, Univ. Alaska, 623 pp, 451–465.
PATTULLO, J.G., 1957: The seasonal heat budget of the oceans. Ph.D. Dissertation, Univ. of California, 104 pp.
PAVLOVA, YU. V., 1966: Seasonal variations of the California Current. *Oceanology*, **6**, 804–814.
POLLARD, RAYMOND T., PETER B. RHINES and RORY O.R.Y. THOMPSON, 1973: The deepening of the wind-mixed layer. *Geophys. Fluid Dynamics*, **3**, 381–404.
RAMAGE, COLIN S., 1970: Meteorology of the South Pacific Tropical and Middle Latitudes. Scientific Exploration of the South Pacific (W.S. Wooster, editor), Nat. Acad. Sciences, Wash., D.C., 257 pp, 16–29.
———, 1975: Preliminary discussion of the meteorology of the 1972–73 El Nino. *Bull. Amer. Meteorol. Soc.*, **56**, 234–242.
——— and T. MURAKAMI, 1973: Comment on the paper by P.R. Rowntree: "The Influence of Tropical East Pacific Ocean Temperatures on the Atmosphere". *Quart. J. Roy. Met. Soc.*, **99**, 393–394.
REID, JOSEPH L., 1973: Northwest Pacific Ocean Waters in winter. The Johns Hopkins Oceanogr. Studies, No. 5, The Johns Hopkins University Press. 96 pp.
ROWNTREE, P.R., 1972: The influence of tropical east Pacific Ocean temperatures on the atmosphere. *Quart. J. Roy. Met. Soc.*, **98**, 290–321.
SCRIPPS INSTITUTION OF OCEANOGRAPHY OF THE UNIVERSITY OF CALIFORNIA, 1962. *Oceanic Observations of the Pacific: 1955* (Editors: Joseph L. Reid, Robert S. Arthur, Edward B. Bennett). Univ. Cal.

Press, 477 pp.
SVERDRUP, H.U., 1957: Oceanography. *Handbuch der Physik*, **48**, Springer-Verlag, Berlin (quoted by Bryan, 1962).
TABATA, S., 1958: Temporal changes of salinity, temperature, and dissolved oxygen content of the water at Station P in the Northeast Pacific Ocean, and some of their determining factors. *J. Fish. Res. Bd. Canada*, **18**, 1073–1124.
———, 1965: Variability of oceanographic conditions of Ocean Station P in the Northeast Pacific Ocean. Trans. Roy. Soc. Canada, Volume 3, Series IV. June 1965. Section 3, 367–418.
———, N.E.J. BOSTON and F.M. BOYCE, 1965: The relation between wind speed and summer isothermal surface layer of water at Ocean Station P in the Eastern Subarctic Pacific Ocean. *J. Geophys. Res.*, **70**, 3867–3878.
TAFT, B.A., 1972: Characteristics of the flow of the Kuroshio south of Japan. Kuroshio, its physical aspects. (Henry Stommel and Kozo Yoshida, editors). Univ. of Tokyo Press, 517 pp, 165–216.
TAKENOUTI, A.Y. and K. OHTANI, 1974: Currents and water masses in the Bering Sea: A review of Japanese work. Oceanography of the Bering Sea, with emphasis on renewable resources. (D.W. Hood and E.J. Kelly, editors), Occasional Publ. No. 2, Inst. of Marine Science, Univ. Alaska, 623 pp, 39–57.
TALJAARD, J.J., H. VAN LOON, H.L. CRUTCHER and R.L. JENNE, 1969: Climate of the upper air, 1, Southern hemisphere, Vol. I, Temperatures, dew points and heights at selected pressure levels. NAVAIR 50-IC-55, 135 pp, U.S. Nav. Weather Service, Washington, D.C.
UDA, MICHITAKA, 1967: Cyclic, correlated occurrence of world-wide anomalous oceanographic phenomena and fisheries condition. *J. Oceanogr. Soc. Japan*, 20th Anniv. Volume, 368–376.
U.S. NAVY HYDROGRAPHIC OFFICE, 1961: Oceanographic Atlas of the Polar Seas, Part I, *Antarctic*, H.O. Publ. 705: 70 pp.
VONDER HAAR, THOMAS H. and ABRAHAM H. OORT, 1973: New estimate of poleward energy transport by Northern Hemisphere Oceans. *J. Phys. Oceanogr.* **3**(2), 169–172.
WEYL, PETER K., 1968: The role of the oceans in climatic change: A theory of the Ice Ages. *Meteorol. Memographs*, **8**, 37–62.
WHITE, W. and A. WALKER, 1973: Meridional atmospheric teleconnections over the North Pacific from 1950–1972. *Monthly Weather Rev.*, **101**, 817–822.
WÜST, G., 1938: *Gerlands Beitr. Geophys.* **54**. (quoted by Deitrich, G., 1963. *General Oceanography*, John Wiley & Sons, Inc., 588 pp.)
WYRTKI, KLAUS, 1965: The average heat balance of the North Pacific Ocean and its relation to ocean circulation. *J. Geophys. Res.*, **70**, 4547–4559.

Evidence of Long Lee Waves in Southern Alberta

Peter F. Lester

Environmental Sciences Centre (Kananaskis)
The University of Calgary
Calgary, Alberta

[Manuscript received 20 October 1975]

ABSTRACT

A brief review of past studies of the chinook and a summary of some recent satellite and visual observations of the chinook arch cloud are presented as evidence of the occurence of long gravity wave phenomena in the lee of the Rockies of Southern Alberta and Northern Montana. A quasi-stationary cloud band that extends several degrees of latitude along the lee of the mountains appears to be associated with a single long wave with a length of the order of 50–100 km or longer, although resonance may be present in some cases. Both satellite and visual observations indicate the frequent occurrence of the wave during the colder period of the year. Taken together, these data imply that the wave phenomenon is potentially important in terms of local surface weather and vertical momentum transport and that it should be subjected to more detailed theoretical and observational studies.

1 Introduction

The chinook of southern Alberta is commonly defined as a warm, dry, gusty wind from the mountains accompanied by rapid temperature changes. It is one of the group of dry downslope winds known more widely as "foehn" (Brinkmann, 1973). It has been described as one of the most important wintertime meteorological phenomena that occur in the area because of its influences on hydrology, agriculture, and the local climatology in general (Marsh, 1965; Longley, 1967). The conceptual model of the chinook that has grown out of past investigations (Osmond, 1941; Godson, 1943; McCabe, 1961; Brinkmann, 1969; Holmes and Hage, 1971) is composed of two major components. On the macroscale, the advection of warm air plays an important role while on the mesoscale, mountain-induced gravity waves modify the larger scale effects. The wide variability of each of these components accounts for the large variations of chinook characteristics. Although many of the properties of the large scale component are well-known, the limited resolution of the conventional meteorological data network has resulted in the neglect of the gravity wave component of the chinook with only a few exceptions (Holmes and Hage, 1971; Kellie, 1972). Brinkmann (1969) has stressed the importance of a better knowledge of the mesoscale structure of the chinook for a complete understanding (and ultimately better predictions) of that phenomenon.

Although the chinook research project at the University of Calgary (Lester, 1975) is currently concentrating its efforts on the macroscale and large-mesoscale characteristics of several chinook situations, high-resolution satellite data have provided information about the smaller-scale wave-structure. The purpose of this paper is to present a synopsis of recent satellite and visual observations and a brief summary of past studies which suggest that the gravity wave component of the chinook is characterized by longer-than-normal lee waves.

2 Past evidence

The idea of long gravity waves in the chinook belt is certainly not new. An early discussion of the chinook by Godson (1943) and work by Hess and Wagner (1948) already hinted at their existence and a recent paper by Wilson (1973) has suggested that mountain-induced gravity-inertia waves may play a role, not only in the production of the chinook but also in the determination of the climatological locations of the lee trough and the Alberta hail maximum.

Fig. 1 Chinook arch as seen from the University of Calgary campus.

The observational evidence suggesting the existence of long lee waves comes from many independent sources. The visual observation of the arch cloud often associated with the chinook is the most frequent indication that a long wave phenomenon is present. The general characteristics of the altocumulus arch cloud (Figure 1) are a sharp western edge and a great cross-wind extent. Reported arch cloud heights generally range between 3500 m and 6500 m AMSL. Thomas (1963) estimated that an 800-km length of the western edge of a typical arch cloud (often reported as standing lenticular – ACSL) could be observed from Calgary, Alberta, at one time. He determined the plan position of the arch from surface observations on one occasion and the diagram he presents bears a striking similarity to satellite observations discussed below. Thomas' observations indicate that the arch cloud is better defined closer to the mountains and it often has an eastward movement. At the latitude of Calgary, the western edge of the arch cloud has a mean position between that city and the mountains (Wilson, 1973). It is not unusual for the more common visual manifestations of the much shorter, ordinary, lee waves (lenticularis and roll clouds) to form at lower levels in the clear area or "window" between the western edge of the arch and the mountains (see Fig. 1) or to be embedded in the arch cloud itself.

Interviews with commercial pilots and forecasters indicate that wave activity is quite common along the airways west of Medicine Hat. Occasional PIREPS serve as good indicators of the character of the wave motion. For example,

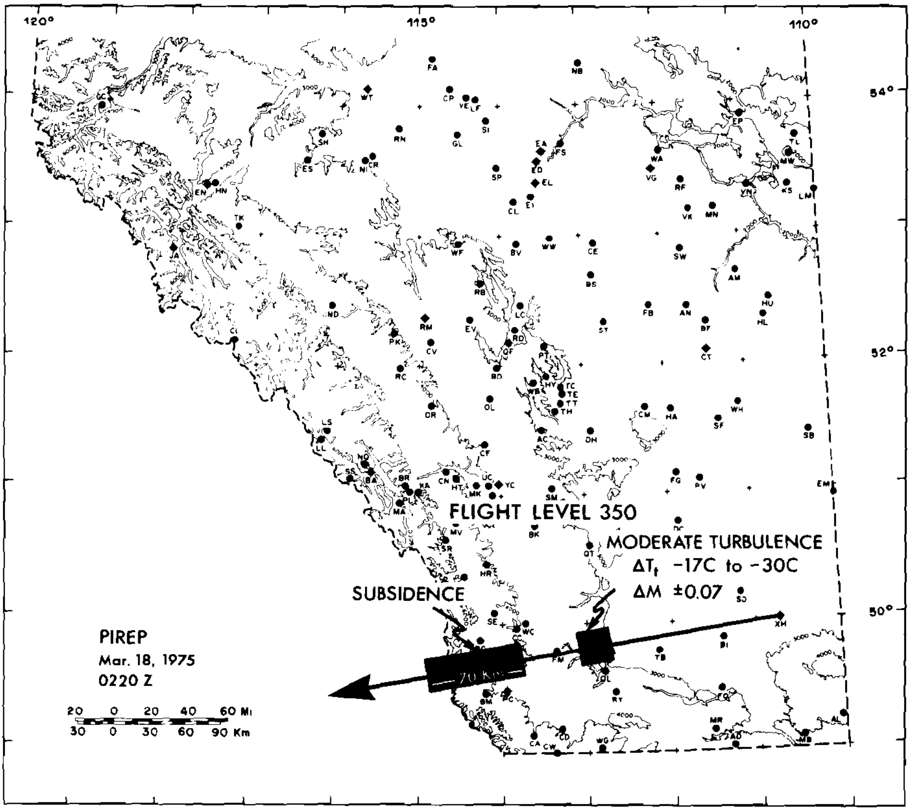

Fig. 2 Commercial jet aircraft pilot report (PIREP) for 0220 GMT, 18 March 1975. ΔT_t and ΔM indicate, respectively, maximum excursions in total temperature and Mach number during turbulence. "Subsidence' is pilot jargon for a smooth downdraft.

Fig. 2 illustrates a recent PIREP which suggests a single wave with a length of over 100 km. Sailplane pilots flying in the southern part of the province have reported resonant waves between the Continental Divide and Medicine Hat with wave lengths of about 60 km. Studies of surface temperature variations at stations between Calgary and Banff (Brinkmann and Ashwell, 1968) imply a wave length of about 70 km during a chinook situation.

Perhaps the most complete long wave observations to date were gathered via aircraft by Holmes and Hage (1971) during chinook conditions. Temperature at several levels up to 1200 m AGL and visual observations of large snow melt areas showed resonance waves of 60–70 km in length. Kellie (1972) has spectrum-analyzed data from two instrumented towers in Calgary to estimate wave lengths in chinook cases. He found eastward progressing waves of the order of 29–118 km in length.

Manson *et al.*, (1974) has published results of wind observations made from Saskatoon, Saskatchewan in the 50–110 km AMSL region with a partial

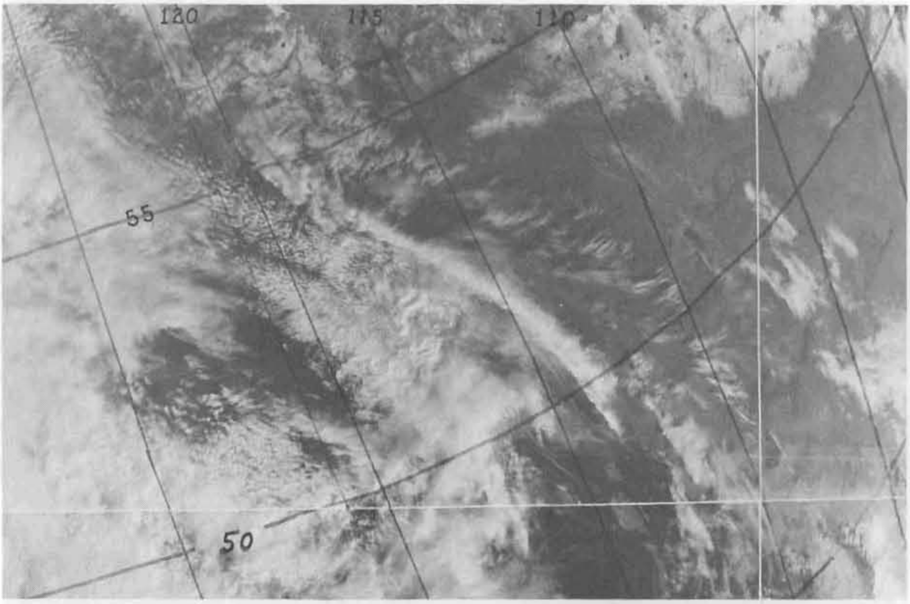

Fig. 3 VHRR Visual image from the NOAA 3 Satellite, 1739 GMT, 1 October 1974. The bright cloud band that crosses 115 W at about 52 N is the arch cloud. Note the much shorter, more common, lee waves visible over the mountains to the west of the arch cloud.

reflection radiowave system. Ray-tracing computations indicated that long (~200 km) gravity waves, associated with measured upper-atmospheric wind fluctuations, were generated in the foothills of the Rockies in central Alberta.

3 Recent evidence

The most recent evidence for the existence of long wave phenomena has come from the chinook project at the University of Calgary. In October, 1974, a chinook "watch" was established. Days on which a chinook arch cloud was observed from the surface were recorded. In a period of six months (through April, 1975) arch clouds were observed from Calgary on 39 days. In an incomplete series of NOAA satellite data for the same period (about forty days of twice-a-day imagery) at least 19 apparent arch clouds have been identified. These data were acquired for periods during which chinook conditions (westerly flow) prevailed at the surface and/or arch clouds were observed from the surface. Two of the better-defined cases are shown in Figs. 3–6. The satellite data examined thus far have revealed the following general characteristics of the arch cloud.

There are two distinct forms: (a) a single, definite cloud band parallel to the mountains with a range of widths from 15 to 200 km (e.g., Fig. 3) and (b) a broad cloud form with a sharp western edge and an ill-defined eastern terminus (e.g., Fig. 5). At the present time, the majority of arch clouds fall into the latter

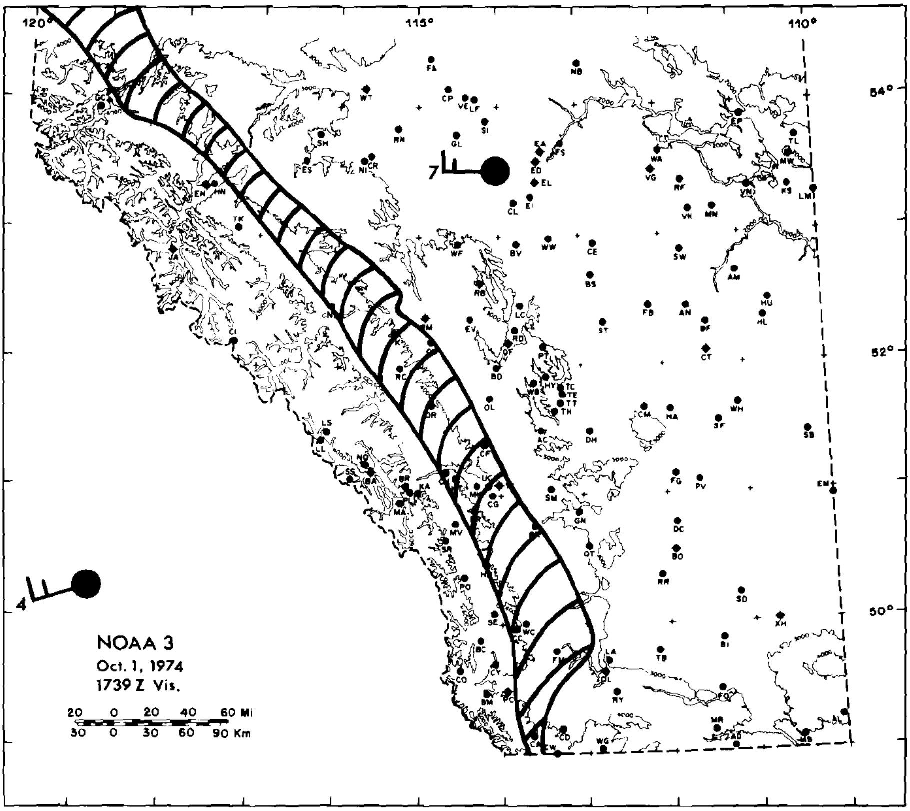

Fig. 4 Schematic representation of arch cloud shown in Fig. 3 over southern Alberta. 500 mb winds at Edmonton and Vernon are shown in ms^{-1}. The heavy dashed line represents the Continental Divide. Surface contours are shown at 2000, 3000, 4000 and 6000 feet AMSL (~ 600, 900, 1200 and 1800 m AMSL).

category. All apparent arches were located east of the major mountain ranges. The cross wind lengths of the observed cloud bands ranged between two and seven degrees of latitude. In all cases the bands occurred in the latitude belt 47 N to 54 N. The usually well-defined western edges of the bands displayed a marked geometric similarity between cases, suggesting a strong tie with the topography. Variations in the orientation of the arch cloud were usually found downstream of major variations in the size or orientation of the mountains. In a number of cases the plan position of the western edge of the arch cloud intersected the Continental Divide at a small angle near latitude 50 N (i.e., the arch cloud was west of the Divide south of that latitude). This suggests that, at least in the southern part of the area, a mountain range west of the Divide was responsible for the flow disturbance. In several cases, arch clouds have been observed to coexist with lower-level bands of clouds which appeared to be associated with "ordinary" lee waves (lengths of the order of 10 km). Most of the cases examined thus far have been associated with only weak to moderate cross-mountain flow at 500 mb (15–20 m s^{-1}).

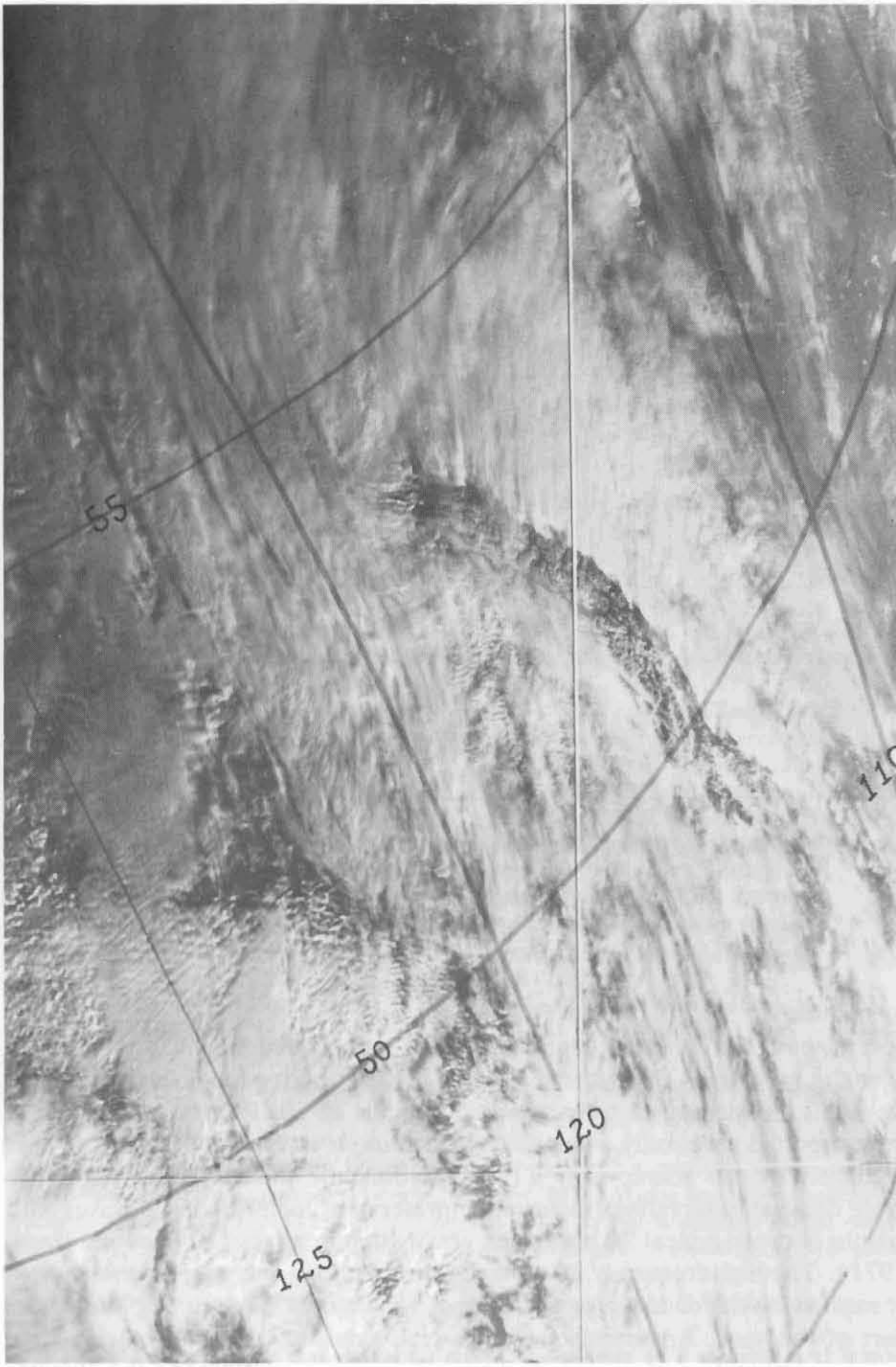

Fig. 5 VHRR Visual image recorded by NOAA 3, 1823 GMT, 30 November 1974. Note that for clarity the 115 W meridian has not been included. The western edge of the arch cloud is visible east of the curved break in the clouds over the Continental Divide.

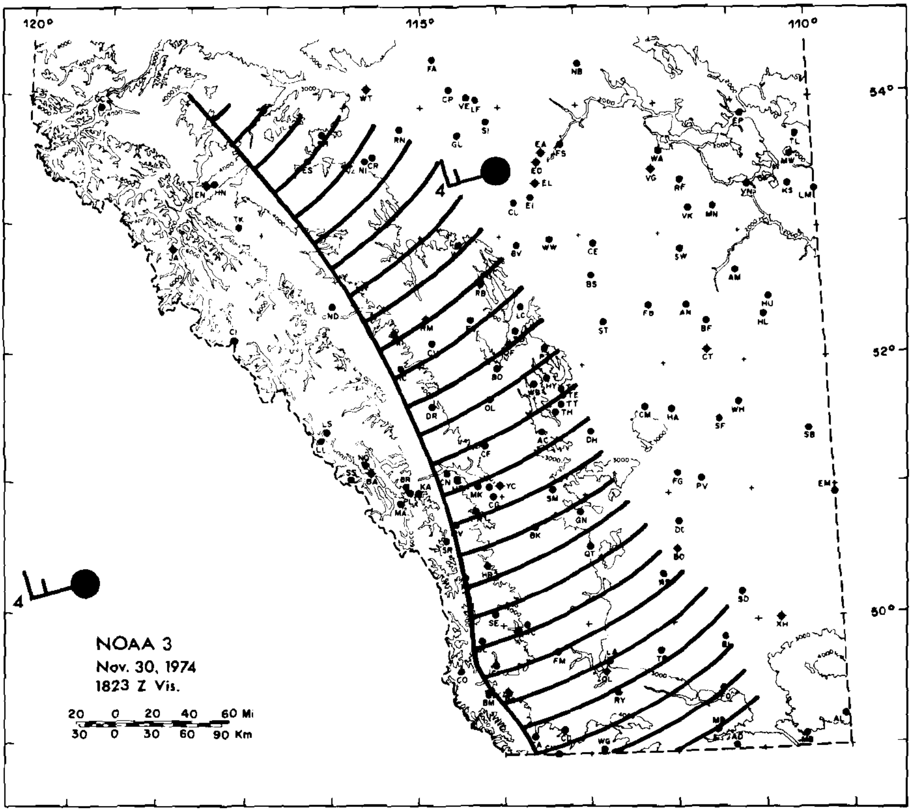

Fig. 6 Schematic of arch cloud shown in Fig. 5. 500 mb winds for Edmonton and Vernon are given in ms^{-1}. Note the tendency for the western edge of the arch cloud to approach the Divide in the south. Also note the sharp break in the curvature of the edge opposite Crowsnest Pass (about 49.7 N).

4 Summary

Several past and on-going chinook studies suggest that stable, westerly flow over the mountains of southern Alberta and northern Montana gives rise to lee-side gravity wave disturbances with lengths of 50–100 km or longer. In most reported cases only a single long wave mode is apparent, similar to that predicted by the Klemp-Lilly (1975) hydrostatic model. However, a few more detailed observations indicate the presence of long resonance waves with lengths between typical lee waves and gravity inertia waves (Holmes and Hage, 1971). The high frequency of occurrence of the long waves over a wide area is implied by the common appearance of the chinook arch during the cooler part of the year. Apparently the large-scale cause of this phenomenon is a unique combination of mountain shape, size and orientation and the climatological state of the westerlies.

Admittedly the evidence presented here is suggestive at best and no firm conclusions can be drawn on the basis of it.[1] However, the possible *climatological* importance of such waves in influencing local weather (Thomas *et al.*, 1974; Webb, 1975), as efficient momentum transport mechanisms (Lilly, 1972) and as coupling mechanisms between the upper and lower atmosphere (Manson *et al.*, 1974) indicates that their role may extend well beyond the local chinook problem. Thus, taken in broader view, these long wave phenomena warrant further investigation to establish clearly their nature and true importance.

Acknowledgements
The author wishes to acknowledge the assistance of the following people during the course of this study: Sharon Gillaspy (NOAA), Katherine Calvert and Della Patton (Environmental Sciences Centre, the University of Calgary). The photograph Mosaic in Fig. 1 was furnished by the Department of Geography, the University of Calgary. Satellite pictures were furnished by the National Environmental Satellite Service, Redwood City, California. This study was partially supported by a subvention from the Atmospheric Environment Service of Canada.

References

BRINKMANN, W., 1969: The definition of the chinook in the Calgary area. Unpublished M.Sc. Thesis, Dept. of Geography, University of Calgary.

———, 1973: A climatological study of strong downslope winds in the Boulder Area, NCAR Cooperative Thesis No. 27, INSTARR occasional paper No. 7, University of Colorado, 229 pp.

BRINKMANN, W., and I.Y. ASHWELL, 1968: The structure and movement of the chinook in Alberta, *Atmos.*, **6**, 1–10.

GODSON, W.L., 1943: A discussion of the chinook arch and chinook winds. Unpublished manuscript, 16 pp.

HESS, S.L., and H. WAGNER, 1948: Atmospheric waves in northwestern United States. *J. Meteor.*, **5**, 1–19.

HOLMES, R.M., and K.D. HAGE, 1971: Airborne observations of three chinook type situations in southern Alberta. *J.Appl. Meteor.*, **10**, 1138–1153.

KELLIE, A.R., 1972: Low level atmospheric structure in Calgary in pre-chinook conditions. Unpublished M.Sc. Thesis, Department of Geography, University of Alberta.

KLEMP, J.B., and D.K. LILLY, 1975: The dynamics of wave-induced downslope winds. *J. Atmos. Sci.*, **32**, 320–339.

LESTER, P.F., 1975: A case study of the Alberta chinook. Paper presented at the ninth congress of the Canadian Meteorological Society, Vancouver, B.C., May 28–30.

LESTER, P.F., and J.I. MACPHERSON, 1975: OPERATION LEECAT. *Atmosphere*, **13**, 126–129.

LILLY, D.K., 1972: Wave momentum flux—a GARP problem. *Bull. Amer. Meteor. Soc.*, **53**, 17–23.

LONGLEY, R.W., 1967: The frequency of winter chinooks in Alberta, *Atmos.*, **5**, 4–16.

MANSON, A.H., J.B. GREGORY, and D.G. STEPHSON, 1974: Winds and wave motions to 110 km at mid-latitudes. I Partial reflection radiowave soundings, 1972–1973. *J. Atmos. Sci.*, **31**, 2207–2215.

MARSH, J.S., 1965: The chinook and its

[1]It should be mentioned that data gathered in the vicinity of a chinook arch cloud during OPERATION LEECAT (Lester and MacPherson, 1975) have shown that the arch cloud was located in the crest of 70–80 km wave in the temperature field. Details of this case will be published elsewhere.

geographic significance in southern Alberta. Unpublished M.Sc. Thesis, Department of Geography, University of Calgary.

MCCABE, H.J., 1961: A new look at chinooks. Dept. Commun. No. 15, Canada Department of Transport, Meteor. Board, Calgary, Alberta, 4 pp.

OSMOND, H.L., 1941: The chinook wind east of the Canadian Rockies, *Can. J. Res.*, **19**, 57–66.

THOMAS, J.E., M.D. KAYS, and J.D. HORN, 1974: Meteorological satellite observations of gravity waves. Preprints of the Sixth Conference on Aerospace and Aeronautical Meteorology, American Meteorological Society, El Paso, Texas, November 12–15, 181–184.

THOMAS, T.M., 1963: Some observations on the chinook 'arch' in western Alberta and northwestern Montana, *Weather*, **18**, 166–170.

WEBB, W.L., 1975: Conference summary—atmospheric gravity wave symposium. *Bull. Amer. Meteor. Soc.*, **56**, 256–257.

WILSON, H.P., 1973: Inertia lee waves and weather in Alberta, Unpublished Manuscript, 11 pp.

On Vertical Interpolation and Truncation in Connexion with Use of Sigma System Models[1]

Hilding Sundqvist[2]

Division de Recherche en Prévision Numérique
Atmospheric Environment Service, Montreal, Quebec

[Manuscript received 26 November 1975; in revised form 10 February 1976]

ABSTRACT

The effect of vertical truncation in connexion with interpolation of geopotential from standard pressure to sigma levels is examined. It is shown that the hydrostatically related temperature and geopotential fields in the sigma system become inconsistently related with regard to calculation of the pressure force in this system. This inconsistency occurs as a result of vertical truncation around temperature inversions (e.g., the tropopause) above a sloping ground. Numerical examples show that erroneous pressure gradients are introduced which, expressed in equivalent gradient wind, have a magnitude of several ms^{-1} in the tropopause region over the Himalayas and the Rocky Mountains.

To avoid those errors, a procedure is developed in which the pressure force, calculated from analyzed geopotentials in the p system, is interpolated to sigma levels.

For consistency, a reversed procedure of the kind just described has to be applied at the end of a forecast when results are to be displayed on pressure surfaces.

The present method has been tested in a few 36-hour forecasts using real data. The results exhibit a noticeable improvement as compared to those obtained when the commonly adopted interpolation scheme is used.

When the pressure force is interpolated, the geopotential fields on the sigma surfaces are obtained by solving a set of vertically coupled elliptic partial differential equations. The problems involved in solving this set by successive over-relaxation (SOR) are analyzed.

1 Introduction

In a recent paper (Sundqvist, 1975b) the author studied in some detail the origin of truncation errors in systems with terrain-following coordinate surfaces – e.g., the sigma- ($\sigma = p/p_s$) system. The investigation focused on the truncation errors of the pressure gradient force and temperature gradient when calculated from discretized functions along σ-surfaces. The temperature, T, and the hydrostatically associated geopotential, Φ, were in that case well defined

[1]Contribution no 319.

[2]Present address: Department of Meteorology, University of Stockholm, Arrhenius Laboratory, Fack, S–104 05 Stockholm, Sweden.

analytical functions of pressure so that any contamination by vertical truncation was excluded. It is also of importance to note that this type of truncation error is repeated at each time step in an integration of the model equations.

A special type of truncation error that shows up in the pressure force as a result of vertical discretization was briefly discussed in the aforesaid paper. This error is introduced only initially in conjunction with interpolation of analysed data from p to σ. A question that we may ask ourselves in that context is namely: in what way shall we try to duplicate the state of the real (or p-system analysed) atmosphere in discretized form in the σ-system? If the most straightforward and common way is chosen, that is, by duplicating the geopotential with the aid of an elaborate interpolation algorithm, then the temperature has to be calculated from the finite difference form of the hydrostatic relation in the σ-system. (Φ and T could of course be interchanged in this reasoning.) As a consequence of vertical truncation, these fields of Φ and T – which both appear in the pressure force terms in the σ-system – are likely to yield a pressure force which deviates from that obtainable directly from the original data at corresponding pressures. Thus, if we consider the pressure force as it is obtained in the p-system to be the correct one, then this way of interpolation from p to σ is likely to introduce an inconsistency between Φ and T which results in an error in the pressure force when this is calculated in the σ-system.

If we interpolate the pressure force instead, we would consequently avoid the error that follows from a possible inconsistency between Φ and T. In such a procedure, however, Φ and T become expressed in terms of differential relations which have to be integrated in order to obtain them explicitly.

This problem of how to arrange the initial data in a consistent way in a σ-type system when the atmospheric state is available in a p-system analysis has also been studied by Phillips (1974). In his paper, Phillips presents in detail a procedure for this purpose, based on energy considerations.

The purpose of the present paper is to explore the above mentioned error that may arise in the initial pressure force as a result of vertical truncation. As a means of avoiding this error, the alternative of interpolating the pressure force instead of Φ (or T) alone will be tested numerically.

A couple of reasons could be mentioned why the p-system structure has been taken as a reference. The most obvious one is that – at least to the author's knowledge – no analyses are presently routinely performed on σ-surfaces.

The relation between Φ and T in the finite difference hydrostatic equation will be discussed in Section 2. A numerical demonstration of the appearance of the pressure force error focused on here is performed in Section 3. A method of interpolating the pressure force and obtaining Φ and T in the σ-system will be developed in Section 4. The two ways of duplicating the initial atmospheric state are then compared in a couple of real data experiments, the results of which are presented in Section 5. Some concluding remarks are then given in Section 6. In the Appendix, the problems of solving the vertically coupled elliptic partial differential equations – derived in Section 4 – by successive overrelaxation (SOR) are analysed.

The model used in the numerical experiments is the PE model of RPN, Atmospheric Environment Service, Montreal, Canada. For reference, see Robert *et al.* (1972). In the present context, it suffices to mention that this model is a hemispheric gridpoint model with five σ-levels: 0.1, 0.3, ..., 0.9.

Although the present investigation mainly centers around a specific PE model design, it is believed that the discussions and results are of general interest because they are applicable to any model that uses a sigma type vertical coordinate.

2 Finite-difference form of the hydrostatic relation

In a discrete vertical representation, the hydrostatic approximation,

$$\frac{\partial \Phi}{\partial \ln p} = \frac{\partial \Phi}{\partial \ln \sigma} = -RT, \tag{1}$$

of course has to be expressed in a finite-difference analogue. In (1) $\sigma = p/p_s$ where p_s is the surface pressure, Φ is the geopotential, T is the temperature and R is the gas constant for dry air. This diagnostic relation has to be applied at each moment (time-step) of the integration of a model with a sigma-type vertical coordinate. The reason for this is that both T and Φ have to be available at the same coordinate level for calculation of the pressure force which reads (in the x-direction):

$$F = \left(\frac{\partial \Phi}{\partial x}\right)_\sigma + RT\,\frac{\partial \ln p_s}{\partial x} \tag{2}$$

in the σ-system. Subscript σ indicates that the differentiation is along constant σ.

The difference approximation of (1) will have a somewhat different formulation depending on whether T is defined only at the σ-levels above the ground, or at all the σ-levels – that is, including $\sigma = 1$. To explain this statement further, let us consider a model with σ-levels k $= 1, 2, ..., N$ where the level N is at $\sigma = 1$. At that level $\Phi_N = \Phi_s$, Φ_s being the geopotential of the earth's surface. Thus, if we regard the first-mentioned alternative in the preceding paragraph, the finite difference approximation (of second-order accuracy) of (1) will have the following form:

$$\frac{s_{k+1}}{s_k(s_k + s_{k+1})}\Phi_{k-1} + \frac{s_k - s_{k+1}}{s_k s_{k+1}}\Phi_k - \frac{s_k}{s_{k+1}(s_k + s_{k+1})}\Phi_{k+1} = RT_k \tag{3}$$

$$\text{for } 2 \leqslant k \leqslant N-1$$

where

$$s_k = \ln \frac{\sigma_k}{\sigma_{k-1}}. \tag{4}$$

Equation (3) cannot be applied at $k = 1$. We rather have to use Φ-values only from $k = 1$ and $k > 1$. (It might, of course, be possible to prescribe a $\Phi_{k=0}$ at

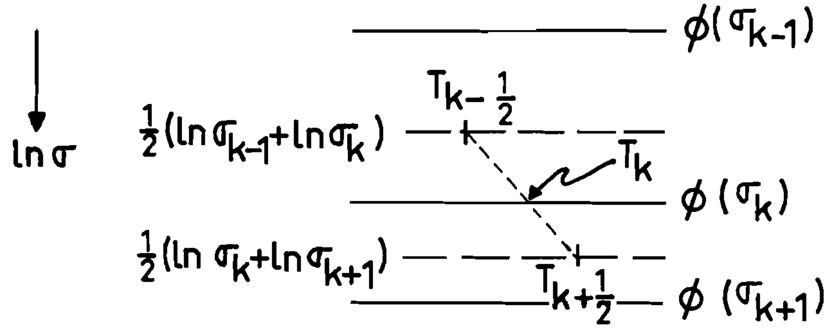

Fig. 1 Illustration of finite difference (second order accuracy) hydrostatic relation between Φ and T.

$\sigma_{k=0}$ well above the top level, $\sigma_{k=1}$ of the model; e.g., by taking the standard atmosphere for $\sigma_{k=0}$.) We will return to this question in a moment.

The meaning of (3) is that we are working with the thickness $(\Phi_{k-1} - \Phi_k)$ and $(\Phi_k - \Phi_{k+1})$ which yield the mean temperatures $T_{k-\frac{1}{2}}$ and $T_{k+\frac{1}{2}}$ for the two layers. Those temperatures are associated with the levels $\ln \sigma_{k-\frac{1}{2}}$ and $\ln \sigma_{k+\frac{1}{2}}$. Then assuming a linear variation in $\ln \sigma$ from $T_{k-\frac{1}{2}}$ to $T_{k+\frac{1}{2}}$ we obtain T_k at $\ln \sigma_k$ as shown in Fig. 1.

We may now more easily explain *a* plausible formulation of the hydrostatic relation for $k = 1$. Namely, we extrapolate through the T-values at $k + \frac{1}{2}$ and $k + 1$ with the assumption that the value of the lapse rate between k and $k + \frac{1}{2}$ is half of that between $k + \frac{1}{2}$ and $k + 1$. Thus

$$T_k = T_{k+\frac{1}{2}} + \tfrac{1}{2}(T_{k+\frac{1}{2}} - T_{k+1}) \tag{5}$$

or in terms of Φ

$$\frac{1}{2}\left(\frac{3}{s_k} - \frac{s_{k+2}}{s_{k+1}(s_{k+1} + s_{k+2})}\right)\Phi_k - \frac{1}{2}\left(\frac{3}{s_k} + \frac{s_{k+1} - s_{k+2}}{s_{k+1}s_{k+2}}\right)\Phi_{k+1}$$
$$+ \frac{1}{2}\frac{s_{k+1}}{s_{k+2}(s_{k+1} + s_{k+2})}\Phi_{k+2} = RT_k; \quad k = 1 \tag{6}$$

When no temperature is defined for $\sigma = 1$ it is natural to work with the thicknesses of the layers. The temperature, which it is necessary to know at the σ-levels for calculation of the pressure force (2), is then determined diagnostically from (3) and (6). This is the way the model is designed that has been used in the present numerical experiments.

Let us for completeness also regard the case in which a temperature is defined at $\sigma = 1$. In this case it is more natural to use the temperature at each σ-level as the prognostic variable. The hydrostatically related geopotential is then obtained by integration of (1) in the discrete system, for example by adopting the trapezoidal approximation

$$\Phi_k = \Phi_{k+1} + \frac{R}{2}(T_k + T_{k+1})s_{k+1}; \quad 1 \leqslant k \leqslant N - 1 \tag{7}$$

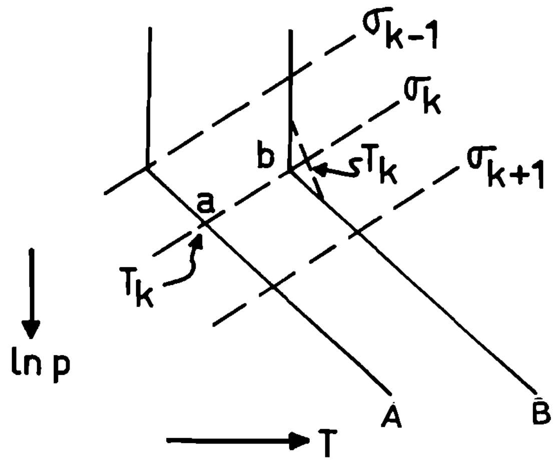

Fig. 2 Illustration of truncation error arising when T is calculated from the finite difference form of the hydrostatic equation (equation (3) in the text) using $\Phi(\sigma)$ as obtained from an analytic expression for $T(p)$.

With the above discussion as a background let us now proceed to a numerical investigation of errors that may arise in the pressure force.

3 Errors arising in the pressure force

As already indicated in the Introduction, we shall assume that the p-system analyses show the "true" state of the atmosphere. Our aim is then to transfer this information to the σ-system as properly as possible by interpolation/extrapolation.

In this section we will investigate what the errors might be if the most straightforward (and common) method of interpolation is adopted, namely interpolation of Φ from p to σ. For this purpose we will consider a case with the well-defined atmospheric state that is characterized by no pressure gradients (except for the hydrostatically balanced part) and no motion.

Let us begin with the following qualitative consideration. Suppose that there are two identical temperature soundings at gridpoints A and B, as shown in Fig. 2, and that we have the analytic expression for $T(p)$. Hence, $\Phi(p)$ is obtained from (1) for any p. Let us furthermore assume that three consecutive σ-levels are distributed and tilted with respect to $p =$ constant as shown in Fig. 2. Then, regard the case in which we have available at the σ-levels the Φ that is compatible with $T(p(\sigma))$ at A and B respectively.

Hence, in order to obtain the correct mean pressure force ($= 0$) with the aid of the σ-system quantities, the average temperature given by $T(a)$ and $T(b)$ (see Fig. 2) *should* be used in (2). However, Φ is given only at discrete σ-points, so we use (3) to calculate temperatures at level σ_k. To find those in Fig. 2 we proceed as described by Fig. 1. The result is that at point A, $T_{Ak} = T(a)$ while at point B, $T_{Bk} \neq T(b)$. Consequently, using T_{Ak} and T_{Bk} for the

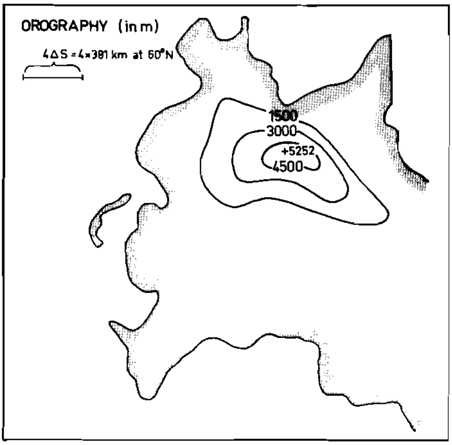

Fig. 3 The model orography over Asia. The labels on the isopleths are in meters.

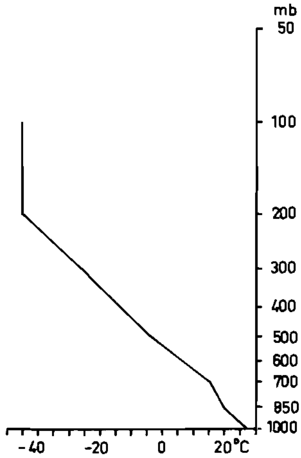

Fig. 4 Stratification used for calculation of the p-system geopotentials.

average temperature in (2) we get a pressure force $\neq 0$. This error in the horizontal pressure force is thus due to a vertical truncation error which yields pairs of (Φ, T) that are inconsistent with respect to the pressure force calculation according to (2). How pronounced this error is, depends on how the σ-levels happen to be situated in relation to possible temperature inversions (e.g., the tropopause) present in the p-system analysis. From (2) we furthermore realize that, for a given temperature discrepancy (in the above case $|T(b) - T_{Bk}|$), the error in the pressure force increases as the magnitude of the individual terms of (2) increase, that is, as the slope of the σ-surfaces steepens.

In Section 4 we will explore a method of eliminating the above type of pressure force error by mutually adjusting Φ and T.

Let us now obtain a more quantitative idea of the pressure force error that arises on a hemispheric grid with the earth's orography included. In Fig. 3 is shown a part covering Asia with the Tibetan and Himalaya mountains, the highest elevations of which are about 5000 m in the model.

We are considering an atmosphere at rest and without horizontal pressure gradients in the p-system. The geopotentials of the standard pressures, 1000, 850, 700, 500, 300, 200, 100 mb, are calculated from the stratification shown in Fig. 4. The pressure at mean sea level (msl) is assumed to be 1000 mb. With this specific choice of the p-system "analysis", we know that the pressure force values that turn out to be non-zero when evaluated in the σ-system are spurious.

The first step of the interpolation procedure is to retrieve the surface pressure, p_s, in the regions where the ground is above msl. In the present model p_s is calculated with the aid of a cubic interpolation, utilizing Φ of the standard p and the ground elevation, Φ_s.

The geopotentials of the five σ-levels are subsequently found by cubic interpolation. At points where $p(\sigma = 0.1) < 100$ mb an extrapolation similar to the one yielding (5) is employed. The temperatures, which are needed in the pressure force term (cf.(2)), are calculated from (3) and (6).

We illustrate possible non-zero pressure gradients in terms of the balanced wind, by solving the balance equation in the σ-system (see Sundqvist, 1975a). The resulting streamfunctions on the five σ-surfaces are depicted in Figures 5a–e over the same region as shown in Fig. 3. The spurious pressure force is rather weak (corresponding to winds $\leqslant 0.5\ \mathrm{m\,s^{-1}}$) at the lower levels where the temperature varies essentially linearly with $\ln p$. At the upper levels, on the other hand, where the interpolated Φ values are directly influenced by the presence of a tropopause in the given p-system data, we find substantial pressure force errors (corresponding to winds $\sim 5 - 10\ \mathrm{m\,s^{-1}}$). The errors at $\sigma = 0.1$ also reflect an uncertainty connected with the extrapolation of information beyond 100 mb.

The scale of the error pattern is of about the same size as the scale of the model orography, which, in this region, indeed is as large as the synoptic scale. Figs. 5a–e furthermore show that the spurious pressure force tends to yield a circulation of opposite sign at adjacent σ-levels. Thus, in case of imbalance between the mass and the wind fields, we may expect long-period internal gravity waves to be set up.

The same qualitative features as those exhibited in Figs. 5 a–e are also found around the Rocky Mountains. The magnitude of the error is smaller, however, as a consequence of less pronounced slopes there; the maximum error corresponds to a wind of about $2\ \mathrm{m\,s^{-1}}$.

Proceeding to the method of interpolating the pressure gradient from p to σ, we may already here note that this method will, in the present case, duplicate the pressure force exactly, as it is zero. Naturally, there will be a certain truncation in a case with a realistic vertical variation of the geostrophic wind. However, the idea with the method is to avoid the error that has been shown above and which is due to an inconsistency between Φ and T.

4 Consistent (Φ, T) pairs obtained from the interpolated pressure gradient

When the pressure gradient is interpolated, the geopotential (and T) on the σ-surfaces is not obtained explicitly, but in differential form. Consequently, we have to solve for Φ (and T) from the information given by the pressure force. This matter will in this section be developed in some detail within the same model design as employed in the preceding section.

The principles of the interpolation procedure are that the pressure gradient components are calculated in the p-system analyses and then interpolated to the σ-levels, where we use the notation

$$\mathbf{F}_p = \nabla_p \Phi \tag{8}$$

for the interpolated pressure force; the aim is then to obtain $\Phi(\sigma)$ and $T(\sigma)$ such that the pressure force

$$\mathbf{F}_\sigma = \nabla_\sigma \Phi + RT\nabla \ln p_s \tag{9}$$

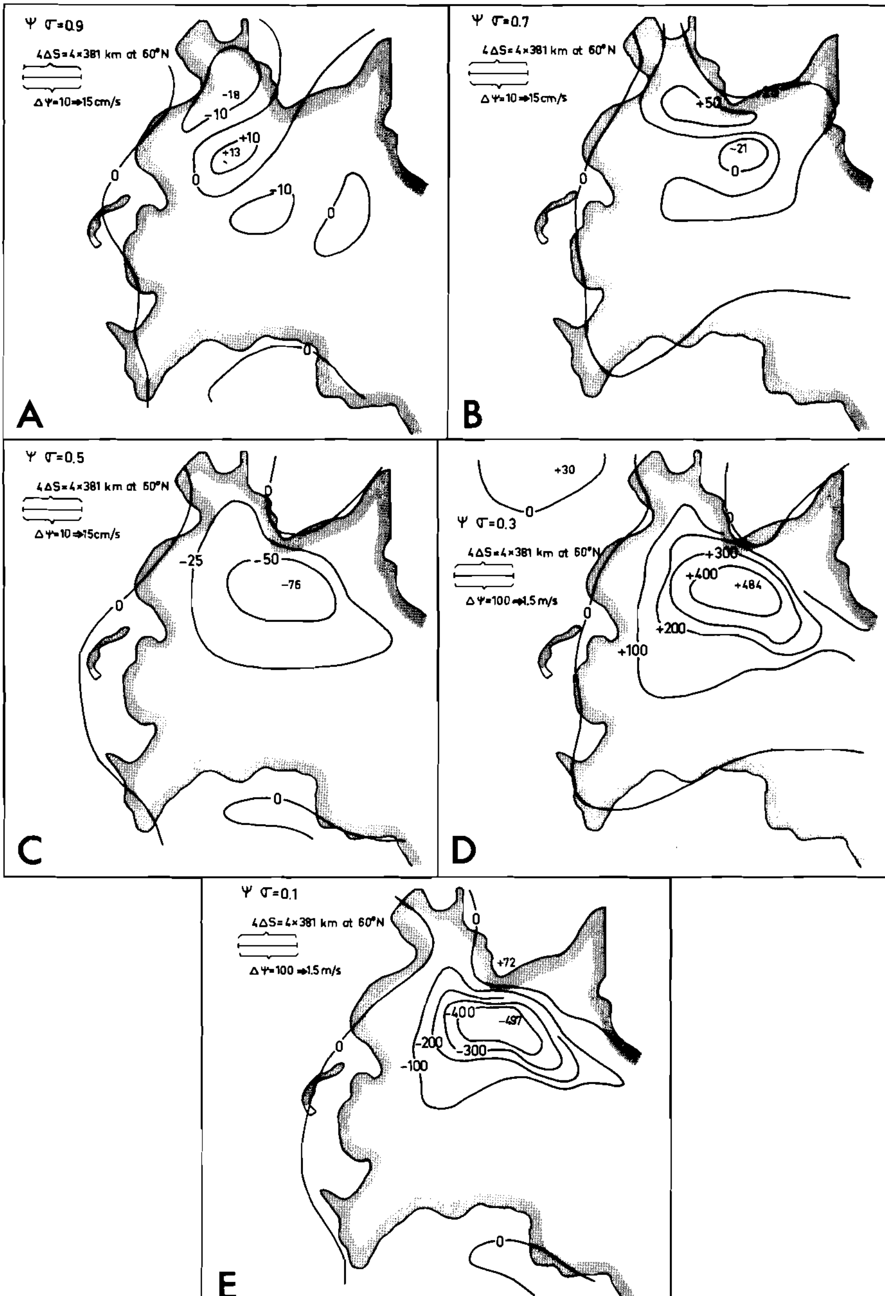

Fig. 5a–e Stream function obtained from the solution of the σ-system balance equation for the case where Φ has been interpolated from the p-system, in which the pressure force is zero. a, ..., e show σ-levels 0.9, ..., 0.1 respectively.

calculated from those quantities equals $\mathbf{F}_p$. In order to get a more convenient equation we equate instead the divergences of (8) and (9). (We also introduce a surface pressure weighting; this has to do with the specific formulation of the right hand side of the balance equation that was used in Section 3.) Hence, our basic equation for obtaining Φ and T at the kth σ-level is:

$$\nabla\cdot[p_s\nabla_\sigma\Phi_k + Rp_sT_k\nabla \ln p_s] = \nabla\cdot(p_s\mathbf{F}_p)_k \tag{10}$$

Writing the hydrostatic relation (3) symbolically as

$$a_k\Phi_{k-1} + (b_k - a_k)\Phi_k - b_k\Phi_{k+1} = RT_k \tag{11}$$

(and an analogous form for (6) and introducing this in (10) we get a Φ-equation that gives the proper pressure force when Φ and T are related via the finite difference form of the hydrostatic equation. For convenience we will write (11) in matrix form

$$\mathbf{A\Phi} = R\mathbf{T} \tag{12}$$

where now $\mathbf{\Phi}$ and $\mathbf{T}$ are column matrices and $\mathbf{A}$ is the coefficient matrix of (3) and (6) together (R is still the gas constant). Thus, we rewrite (10):

$$\nabla\cdot[p_s\nabla_\sigma\mathbf{\Phi} + \mathbf{A\Phi}(p_s\nabla \ln p_s)] = \mathbf{D}_p \tag{13}$$

$\mathbf{D}_p$ being the column matrix of the rhs of (10).

In order to solve the elliptic equation (13) we must know $\mathbf{\Phi}$ on the boundaries. So there we resort to $\mathbf{\Phi}$ obtained from the interpolation as it is described in Section 3. The kind of inconsistency error that we are considering may be minimized in the boundary values by making the model orography equal to zero in a strip along the boundary.

In the present study, we will solve for the necessary correction, $\boldsymbol{\varphi}$, to the geopotential, $\mathbf{\Phi}^{(1)}$, in order to satisfy (13); $\mathbf{\Phi}^{(1)}$ being obtained by the interpolation procedure that is described in Section 3. That is, we evaluate the column matrix

$$\mathbf{D}^{(1)} = \nabla\cdot[p_s\nabla_\sigma\mathbf{\Phi}^{(1)} + \mathbf{A\Phi}^{(1)}(p_s\nabla \ln p_s)] \tag{14}$$

and with $\mathbf{\Phi} = \mathbf{\Phi}^{(1)} + \boldsymbol{\varphi}$ inserted in (13) we have

$$\nabla\cdot[p_s\nabla_\sigma\boldsymbol{\varphi} + \mathbf{A}\boldsymbol{\varphi}(p_s\nabla \ln p_s)] = \mathbf{D}_p - \mathbf{D}^{(1)} \tag{15}$$

with the boundary condition $\boldsymbol{\varphi} \equiv 0$.

With regard to solving the three-dimensional equation (15), this is encumbered with a complication because of the structure of the second term. A more detailed analysis of this matter is given in the Appendix.

The present interpolation method was applied to the case that was investigated in Section 3 (i.e., $\mathbf{D}_p \equiv 0$). The resulting correction $\boldsymbol{\varphi}$ on the five σ-levels is depicted in Figs. 6 a–e over the same region as shown in Figs. 5 a–e. In the lower layers the required corrections are quite moderate, while they are substantial in the upper two layers in which the p-system tropopause is situated.

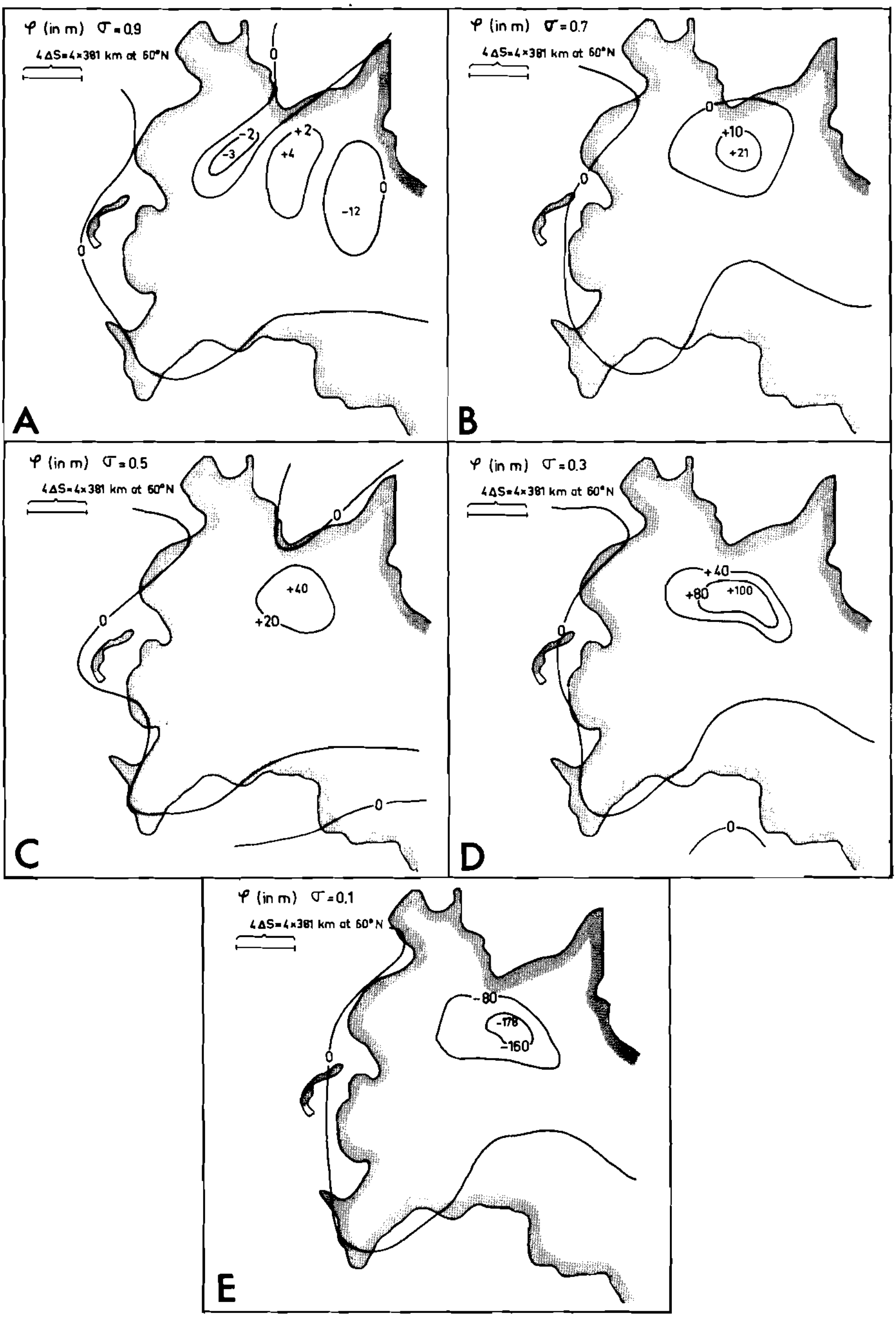

Fig. 6a–e Difference φ between Φ, obtained from the interpolated pressure gradient, and interpolated Φ. a, ..., e show σ-levels 0.9, ..., 0.1 respectively.

To check the pressure force as it is obtained from Φ (= $\Phi^{(1)}$ + φ and the associated T (equations (3) and (6)), the balance equation was applied using these new (Φ; T) pairs in the forcing terms. The results reveal that the pressure force errors, in terms of the balanced wind, have a magnitude that is less than 0.5–0.6 m s^{-1} everywhere. It may be noted that in the study (Sundqvist, 1975b) of the pressure force error that is a consequence of the spectral distribution of Φ and T along σ-surfaces, it was concluded that a maximum error of that magnitude is practically unavoidable in a σ-system model with a realistic orography included. On the other hand, this magnitude seems to be acceptable. It is also worth remarking that the error due to horizontal truncation thus contributes with merely this magnitude to the errors demonstrated in Section 3.

5 Comparison between the two methods of interpolation, using real data

When verifying (and displaying as well) real data forecasts made in a σ-system model, it is convenient to first interpolate Φ from σ to p. Now, when the method of interpolating the pressure gradient of the initial fields is employed, this implies that we have made no effort to duplicate the geopotential itself, but rather the pressure force. Therefore, at the end of a forecast, the reversed procedure has to be applied for consistency. Thus, in that case, Φ on the standard p-levels is obtained by solving a Poisson equation at each level.

Regardless of what the interpolation method is, there is a particular problem of assessing reasonable values for standard pressure levels (mainly 1000 and 850 mb) that are below the ground and for which an extrapolation has to be used. As apparent forecast errors at these levels may substantially be due to those circumstances, the 1000 mb level is excluded in the comparisons to be presented below.

The PE model mentioned in the Introduction was used in the 36-h prognoses that are compared. We will present quantitatively the results of two cases (initial times 1974-01-16 and 1974-05-18) in which the ordinary forecasts showed somewhat less skill than in the average. Let us denote by A the method where Φ is interpolated and by B the method where the pressure gradient is interpolated.

Table 1 shows the difference of the rms error of Φ, (A − B), in m at 36 h. The numbers are averages from six different verification areas, all north of about 25–30° latitude. A clear improvement of the forecast height field in terms of rms error is found when the method of interpolating the pressure gradient is employed in the process of arranging the initial mass field.

The same characteristics are noticed in the S1 skill scores that are also presented in Table 1. The values yielded by B are markedly better than those originating from A. Experience has generally shown that S1-values very much reflect the smoothness of a forecast field; the smoother the field the better (i.e., smaller) the S1 score. In the present cases, this does not mean that lows and highs are generally more smoothed in case B than in A. It is rather an over-all

TABLE 1. rms error difference (A − B) in m and the S1 skill score for A and B.

Pressure →		850	700	500	300	200	100
rms difference	16/1–74	1.06	−0.0	2.73	1.03	4.55	1.95
	18/5–74	1.94	0.98	1.53	0.28	1.25	0.97
S1 score, 16/1–74	A	0.68	0.65	0.58	0.56	0.54	0.52
	B	0.60	0.58	0.51	0.50	0.46	0.51
S1 score, 18/5–74	A	0.75	0.69	0.62	0.60	0.64	0.83
	B	0.67	0.63	0.56	0.53	0.55	0.84

smoothness of the height fields that stands out in B. In limited regions of the forecast Φ-fields of A, short wave ($\sim$3–4 Δs) noise appears while such features are hardly discerned in B.

These two comparative experiments may be too few to draw definite conclusions from. Nevertheless the comparisons do indicate a (nearly) systematic improvement of the forecasts when the pressure gradient information—instead of Φ itself—is transferred from p to σ in the initial fields.

In the present study no attention has been paid to minimizing the additional computing time that follows with the suggested procedure. The impression is that, with a well optimized program, the addition would amount to about 10–15% of the time for a 36-h forecast starting from the p-system analyses. This figure is probably not generally valid since it is likely to depend on the capacity and design of the computer system being used.

6 Concluding remarks

When a transformation to a terrain-following coordinate system is performed, the pressure gradient becomes expressed by the sum of two terms, the magnitude of which is small compared to that of the individual terms in mountainous regions. (A corresponding effect also appears in the z- and the p-systems when the orography is included; see e.g., Katayama *et al.*, 1974). Truncation effects on Φ and T individually are not necessarily troublesome, but because of an inconsistent effect on the two pressure force terms, the truncation may have a relatively strong impact on the net of those terms. The truncation that appears as a consequence of the spectral distribution along σ-surfaces causes an error that is repeated at each time step. These circumstances were explored in Sundqvist (1975b). In the present study it has been found that an error in the pressure gradient may arise in the *initial* fields as a result of vertical truncation occurring in connection with the interpolation from the p-system to a σ-type system. Furthermore, the quantitative examination shows that this error has roughly the same scale as the model orography and that the magnitude may be quite appreciable, namely about 5–10 m s^{-1} in terms of a balancing gradient wind in the layers around pronounced inversions like the tropopause.

We have suggested and tested the method of interpolating the pressure gradient as a remedy to the problem under consideration. The objective of this method is to obtain the best possible duplication of the analysed pressure force. Consistent pairs of (Φ; T) are then obtainable from the given pressure gradient field in the system with terrain-following coordinate surfaces. In solving for Φ and T, these are related via the hydrostatic equation in finite difference form in that coordinate system. Results from numerical applications on real data forecasts indicate that improvements that are not negligible may be achieved with this method.

The kind of pressure gradient error that we have investigated might also have a degrading effect in a p-system objective analysis cycle that contains a σ-type PE model for providing the first guess fields. The interpolation to the σ-coordinates may introduce spurious pressure gradients in the initial fields for the forecast model. The possible errors then arising in the subsequent forecast may be retained over appreciable periods of time (several cycles in the continuous objective analysis process) in areas like the mountainous Tibetan regions. This problem seems to deserve some attention and comparative experiments ought to be made.

An efficient way of generally suppressing this particular type of error would be, of course, to perform the analyses in the coordinate system that is being employed in the prognostic model system in question. Such an approach would, however, require an extensive treatment of data to assess necessary statistical parameters—which would probably be applicable to a specific model design only. However, in several types of four-dimensional data assimilation experiments, it appears to be a feasible undertaking to take due regard to the problem directly in the model coordinate system.

Acknowledgement

The present study was done during the author's stay at the Division de Recherche en Prévision Numérique (RPN) of Atmospheric Environment Service, Canada under contract no. OSV3-0262.

The figures have been drafted and the manuscript typed at the Department of Meteorology, University of Stockholm, Sweden.

Appendix

We will here examine equation (15) of Section 4 as to a necessary condition for convergence when successive over-relaxation is employed for solving the equation on a cartesian grid. We will not derive a stringent formulation of such a condition, but rather a fairly qualitative one. Nevertheless, this appears to give adequate guidance for a practical procedure.

Let us neglect the weighting by the surface pressure and then regard the equation

$$\nabla^2\varphi + \nabla(\mathbf{A}\varphi\nabla z_s) = \mathbf{D} \tag{A1}$$

which is principally the same as equation (15). The field z_s ($= \ln p_s$) has a pronounced variation in mountainous regions and this is the cause of the complication of the problem. The elements of the square matrix $\mathbf{A}$ are those given by equations (3) and (6) of Section 2. As **A** is independent of the horizontal coordinates (x, y) we may conveniently separate the variables and instead consider an equation corresponding to (A1) for each vertical mode. Hence, we introduce the eigen-values, λ_m, of **A** and the associated column eigen-vectors $\boldsymbol{\Psi}_m(x, y)$ and get

$$\nabla^2 \boldsymbol{\Psi}_m + \lambda_m \nabla \cdot (\boldsymbol{\Psi}_m \nabla z_s) = \mathbf{d}_m \tag{A2}$$

Equation (A2) is obtained from (A1) by pre-multiplying with the square matrix **B**, the rows of which are the row eigen-vectors of **A**. We furthermore introduce the two square matrices **C**, the columns of which are the $\boldsymbol{\Psi}_m$, and **M**, the diagonal elements of which are the λ_m, all other elements being zero. Then we have the closing relations

$$\mathbf{BC} = \mathbf{I} \quad \text{(the unit matrix)} \tag{A3}$$

$$\mathbf{CMB} = \mathbf{A} \tag{A4}$$

Returning to (A2), in order to simplify the discussion, we assume that there are no variations in the y-direction. For convenience we write the finite difference form of this simplified version of (A2) in matrix form

$$(\mathbf{L} - \mathbf{I} + \mathbf{U})\boldsymbol{\Psi}_m = \mathbf{d}_m \tag{A5}$$

where **L** and **U** have non-zero elements only below and above the diagonal respectively. With second order accuracy differences the elements of **L** and **U** are

$$\frac{1 \pm \frac{\lambda_m}{2}(z_{si} - z_{si+1})}{2 - \frac{\lambda_m}{2}(z_{si+1} + z_{si-1} - 2z_{si})} \tag{A6}$$

where + applies to **U** and − to **L**.

The sequential relaxation used for solving (A5) is expressed as (with over-relaxation coefficient = 1)

$$(\mathbf{L} - \mathbf{I})\boldsymbol{\Psi}_m^{\nu+1} = \mathbf{d}_m - \mathbf{U}\boldsymbol{\Psi}_m^{\nu} \tag{A7}$$

where ν is the iteration number. Subtracting (A5) from (A7) and denoting the error vector by

$$\boldsymbol{\varepsilon}^{\nu} = \boldsymbol{\Psi}_m^{\nu} - \boldsymbol{\Psi}_m$$

we get

$$(\mathbf{L} - \mathbf{I})\boldsymbol{\varepsilon}^{\nu+1} = -\mathbf{U}\boldsymbol{\varepsilon}^{\nu}$$

or

$$\boldsymbol{\varepsilon}^{\nu} = -(\mathbf{L} - \mathbf{I})^{-1}\mathbf{U}\boldsymbol{\varepsilon}^{\nu-1}$$

and in terms of the first guess error vector $\boldsymbol{\varepsilon}^0$

$$\boldsymbol{\varepsilon}^{\nu} = (-1)^{\nu}[(\mathbf{L} - \mathbf{I})^{-1}\mathbf{U}]^{\nu}\boldsymbol{\varepsilon}^0 \tag{A8}$$

Thus we find the general condition for convergence in this kind of relaxation process, namely that all eigen-values, μ, of the matrix $(\mathbf{L} - \mathbf{I})^{-1}\mathbf{U}$ have magnitudes less than unity. Since $\mu = \mu(\lambda_m)$, $|\mu| < 1$ implies that there is a constraint put on λ_m. From (A6) we may intuitively realize that for large $|\lambda_m|$ the denominator might become too small in regions where the curvature in z_s is markedly positive, that is, around the summits of mountains.

To obtain some further specification of these matters, a numerical example of the above steps was set up for a (5×5) matrix. First the λ_m were calculated according to the coefficients of (3) and (6) in Section 2 for a five-level model. One $|\lambda|$ turns out to be noticeably greater than the others. This is a consequence of the difference in $\Delta\sigma$ steps around $\sigma = 0.9$ – downwards $\Delta\sigma = 0.1$ and upwards $\Delta\sigma = 0.2$.

The maximum of the z_s-terms in (A6) (with $\lambda_m = 1$) as well as (A8) itself was calculated from the model orography. With the values so obtained, the eigenvalues $\mu(|\lambda|_{\max})$ were computed, and it was found that some $|\mu|$ were > 1.

The coefficient of Φ_k in (3) at $\sigma = 0.9$ was then changed by imposing a smaller value, and λ_m subsequently re-calculated. These experiments showed that when $|\lambda_m|$ all are smaller than a certain value, also all $|\mu|$ are < 1.

The coefficients of equations (3) and (6) (i.e., the elements of **A**) are functions of the vertical grid and thus fixed quantities once the vertical subdivision is decided. So, what does it mean when we change the value of the coefficient in question? Let us first state that it is hardly conceivable to change the surface pressure field (i.e., z_s in A6) in order to achieve the desired effects, because such a change would move the positions of all the σ-levels. We shall also recall that strictly $\varphi_N \equiv 0$, that is, no changes in the orography. None the less it appears quite plausible to relax this boundary condition by prescribing

$$\varphi_N = \beta\varphi_{N-1} \tag{A9}$$

This condition implies (with $0 < \beta < 1$) that the thickness changes of the lowest layer are not allowed to be as large as ϕ_{N-1} alone would render.

The coefficient $(b_k - a_k)$ for Φ_k at $\sigma = 0.9$ now becomes (see equations (3) and (11))

$$(b_k - a_k) = \frac{s_k - s_{k+1}}{s_k s_{k+1}} - \beta\frac{s_k}{s_{k+1}(s_k + s_{k+1})}; \quad k = N - 1 \tag{A10}$$

A suitable value of β will give a $(b_k - a_k)$ such that all $|\lambda_m|$ become sufficiently small. The precise β-value to be used will depend on horizontal resolution and on how pronounced the orographic (i.e., z_s) variations are within the grid of a specific model. Naturally, with a non-zero β, the change according to (A9) has to be put on the orography for consistency.

In the experiments presented in Sections 4–5 we had $\beta = 1 - (s_{k+1}/s_k)^2 \simeq 0.82$ in the present resolution. This β-value makes $a_k = b_k$ for $k = N - 1$. We then realize from Fig. 6a that the change of the orographic field is nowhere more than 3–4 m.

One experiment has been run in which β had a smaller value, just sufficient to ensure convergence and it was found that the resulting φ-fields differed insignificantly from the earlier ones.

References

KATAYAMA, A., Y. KIKUCHI, and Y. TAKIGAWA, 1974: MRI Global 3-level model. GARP Publications Series No. 14, 174–188.

PHILLIPS, N.A., 1974: Application of Arakawa's energy-conserving layer model to operational numerical weather prediction. US Dept. of Commerce, NMC, Office Note 104.

ROBERT, A., J. HENDERSON, C. TURNBULL, 1972: An implicit time integration scheme for baroclinic models of the atmosphere. *Monthly Weather Review*, **100**, 329–335.

SUNDQVIST, H., 1975a: Initialization for models using sigma as the vertical coordinate. *J. Appl. Meteor.*, **14**, 153–158.

———, 1975b. On truncation errors in sigma-system models. *Atmosphere*, **13**, 81–95.

A NOTE ON MINIMUM TEMPERATURE AND THE CLIMATOLOGICAL DAY AT FIRST ORDER STATIONS

A. Bootsma

P.E.I. Department of Agriculture and Forestry
Charlottetown, P.E.I.

[Manuscript received 9 December 1975; in revised form 6 February 1976]

The measurement of daily minimum air temperature is an important aspect of weather monitoring in Canada. Long term records of minimum temperature often form an integral part of regional climatic classification for agriculture, forestry and tourism among others.

First order or principal weather stations operated by the Atmospheric Environment Service in Canada presently follow World Meteorological Organization guidelines with respect to minimum temperature by adhering to a climatological day which ends at 0600 GMT, corresponding to 0200 AST in the Maritimes (Canada, Atmospheric Environment Service, 1970). Meanwhile, ordinary climatological stations with two readings daily follow a climatological

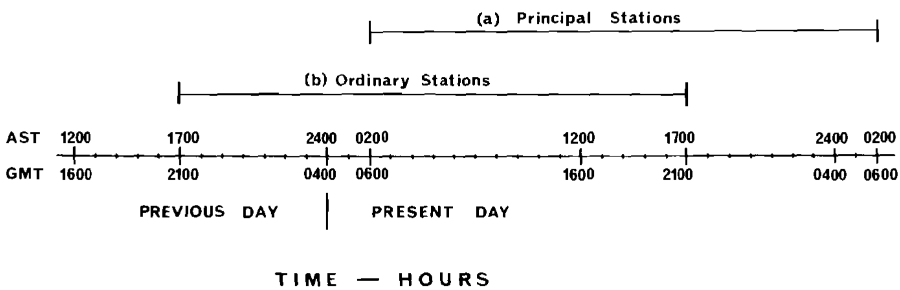

Fig. 1 Climatological day for minimum temperature in effect at (a) Principal stations (from 0600 GMT or 0200 AST of present day); (b) Ordinary climatological stations (from 1700 LST of previous day).

day which begins approximately 1700 LST on the previous day and ends on 1700 LST of the present day (Canada, Meteorological Branch, 1965). The difference between these two climatological days is depicted more clearly in Fig. 1. We have found that significantly different daily minimum temperatures are frequently recorded as a result of these two practices.

Burrows (1964) suggested that differences in minimum temperature due to the variation in climatological day are infrequent and only occur if the minimum temperature falls between the late afternoon observation at ordinary stations

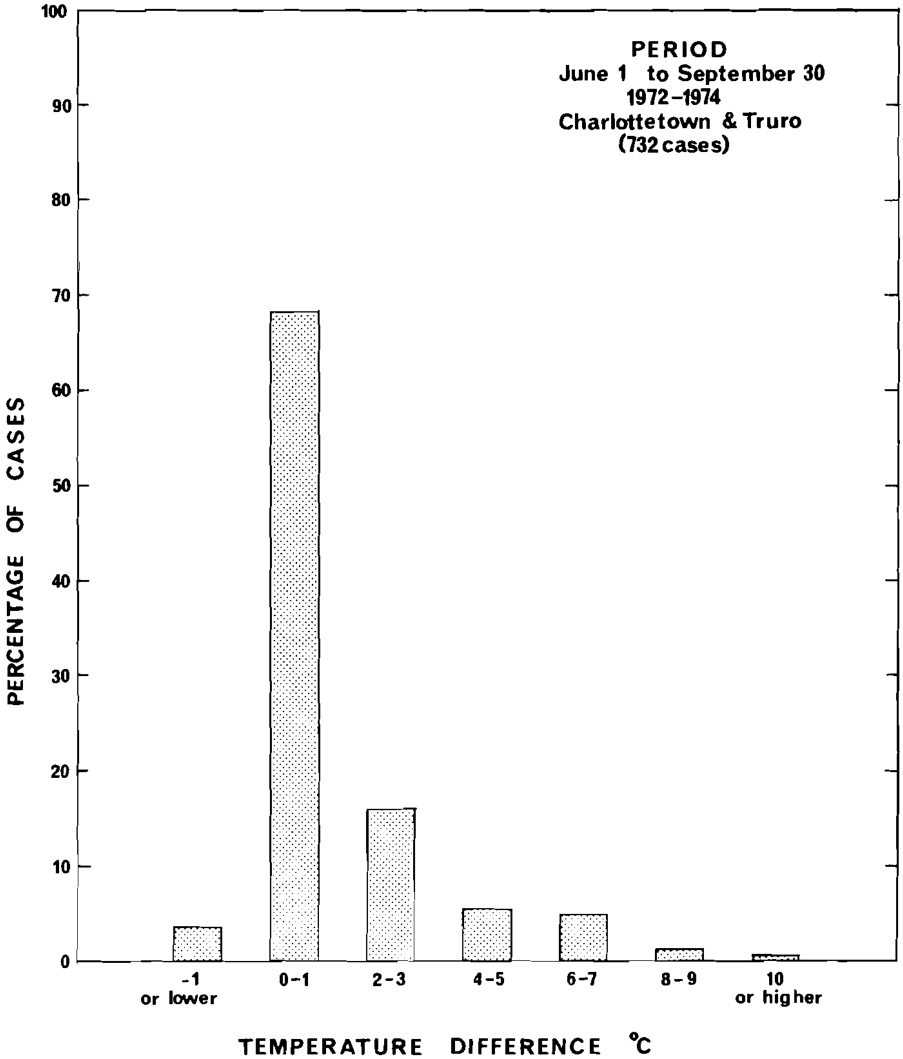

Fig. 2 Frequency distribution of minimum temperature differences arising from different climatological days at ordinary and first order stations.

and the following 0600 GMT observation, although no data were presented to support this. Our experiences indicate that serious and frequent differences occur when a moderately warm night is followed by a night with relatively cooler temperatures even though the minimum occurs after the 0600 GMT (0200 AST) observation. Under these circumstances the temperature prior to 0600 GMT on the cool night may be considerably lower than the minimum on the previous night. As a result, the temperatures that are entered on the climatological summary for two consecutive days actually occur on the coldest of the two nights and only several hours apart. Consequently a climatological day ending 0600 GMT underestimates the actual mean minimum temperature for the month.

TABLE 1. Estimated error in monthly mean minimum temperature (°C) at first order stations (1972–1974 average).

	June	July	August	September
Charlottetown, P.E.I.	0.9	1.2	1.4	1.5
Truro, N.S.	0.8	0.7	1.2	1.7

Hourly and synoptic records at Truro, Nova Scotia, and Charlottetown, P.E.I. for the months of June through September, 1972 to 1974, were examined to determine the frequency and size of the errors involved. Minimum temperatures determined for a climatological day ending at the 1800 GMT synoptic hour were compared with the minimum temperatures entered on the climatological summary for these first order stations. The 1800 GMT synoptic hour was selected because it occurs the closest to the climatological day in effect at ordinary stations in the Maritimes.

Fig. 2 demonstrates the size of the differences involved and the frequency with which they occur. Although the differences were less than 1 °C in 71% of the 732 cases examined, 63 cases had differences of 5 °C or more. Table 1 demonstrates that the climatological day in effect at first order stations underestimates the monthly mean minimum temperature by as much as 1.7 °C. The differences appear to be largest during the cooling-off portion of the growing season. The temperature differences represented an average of 66 units in the accumulated growing degree-days (above 5 °C) from June 1 to September 30, or about 5% of the seasonal degree-day summations.

These results suggest that a more complete documentation of differences in minimum temperature arising from different climatological days is needed for all first order stations in Canada and all seasons of the year. Meanwhile, some caution should be used when interpreting minimum temperatures and derived parameters from first order stations. A more suitable practice of ending the climatological day for minimum temperature at the synoptic hour which corresponds most closely to the climatological day at ordinary stations is suggested since the air temperature is not likely to be near its lowest value for the day at that time. In the Maritimes this would correspond to the 1800 GMT (1400 LST) synoptic hour but may be different for other time zones in Canada.

References

BURROWS, W.R., 1964: Differences in temperature data from ordinary climatological stations arising from once daily readings as compared to twice daily readings. Canada, Dept. of Transport, Meteorol. Branch, CIR 3963, TEC 498.

CANADA, ATMOSPHERIC ENVIRONMENT SERVICE, 1970: *MANOBS*, Manual of standard procedures for surface weather observing and reporting. Dept. of Environment, Atm. Env. Ser., 6th Edition, UDC: 551·501·1.

CANADA, METEOROLOGICAL BRANCH, 1965: Card Type-4, card format documentation. Dept. of Transport, Meteorol. Branch, Toronto.

THE ROUND LAKE

Henry W. Brandli[1] and John W. Orndorff[2]
Detachment 11, 2 Weather Squadron, Air Weather Service, Patrick Air Force Base, Florida

[Manuscript received 17 February 1976]

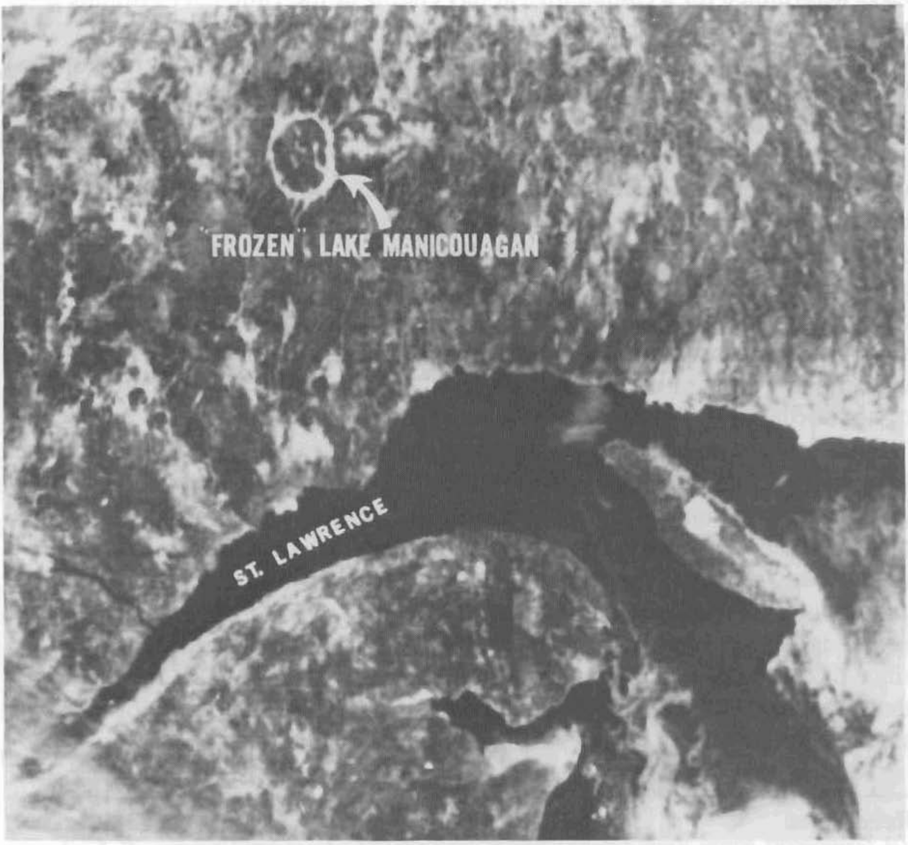

Fig. 1 Lake Manicouagan. Defense Meteorological Satellite Program (DMSP) (0.62 km) resolution, February 1975.

On the above picture (Fig. 1), north of the St. Lawrence Estuary, you will see a white ring. This visual picture is a Defense Meteorological Satellite Program (DMSP), 0.62 km resolution, product taken during February 1975.

[1]Lt Colonel, USAF.
[2]Major, USAF.

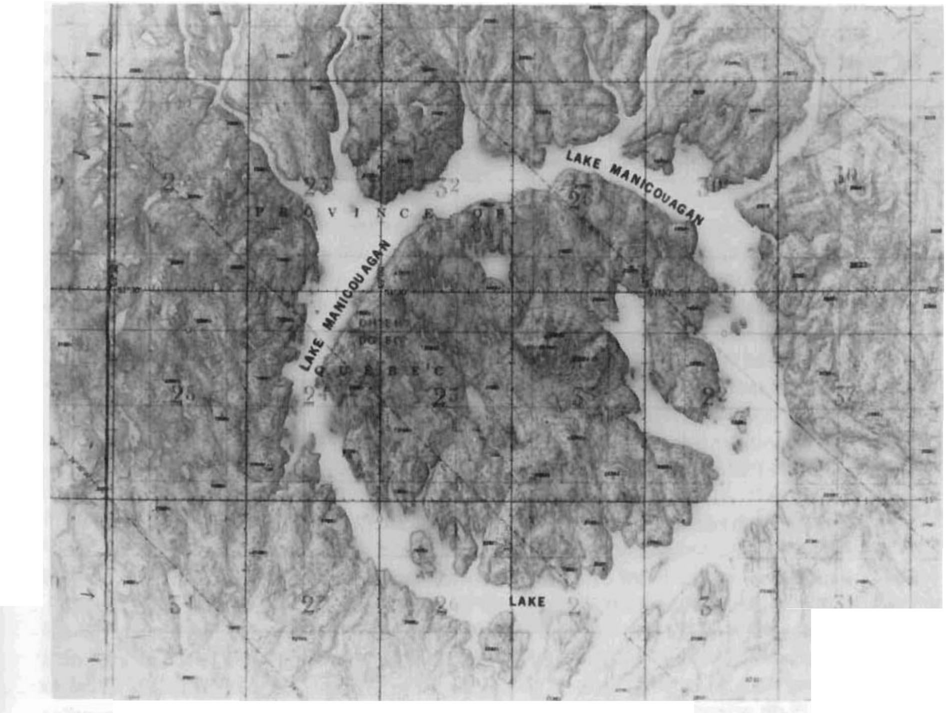

Fig. 2 Lake Manicouagan. Joint Operations Graphic (Air) Map, 1971.

The white ring is frozen Lake Manicouagan, Province of Quebec, Canada, surrounding an extremely large island. This island has two mountain tops in excess of 910 m. Note the various rivers flowing into the lake. The second picture (Fig. 2) is a Joint Operations Graphic (Air) map, printed during 1971. Lake Manicouagan is located approximately 51°15′N 68°45′W and is roughly 108 km in diameter. This lake has been an important landmark in gridding meteorological satellite images with regard to the accurate placing of latitude and longitude lines on the imagery.

CLOUD PHYSICS AND WEATHER MODIFICATION. Yu. S. Sedunov, Editor. Keter Publishing House Jerusalem Ltd., Jerusalem, 1974, 106 pp, hardcover. Available in U.S. and Canada from International Scholarly Book Services, P.O. Box 4347, Portland, Oregon 97208, U.S. $14.00.

This volume is a translation of Proceedings No. 19 of the Institute of Experimental Meteorology of the Main Administration of the Hydrometeorological Service, Moscow. Originally published in 1970, it is a collection of five papers on cloud physics or weather modification and as such is somewhat misleadingly titled in the English version. A more appropriate title would have been "Selected Topics in Cloud Physics" or, as in the original, "Problems in Cloud Physics and Weather Modification".

The collection consists of the following papers:

Yu. S. Sedunov: Cloud physics and weather modification research in the USA.

I.V. Litvinov: Modification of clouds and precipitation in central European USSR.

E.L. Aleksandrov: Measurement of condensation nuclei and cloud nuclei concentrations (a survey).

V.M. Voloshchuk: Hydrodynamic aspects of aerosol particle coagulation theory.

S.P. Belyaev: Use of intermittent illumination in aerosol research.

Dr. Sedunov was with a team of Soviet scientists who visited the United States in 1969 to become acquainted with American research in cloud physics and weather modification. The team visited a number of university and government laboratories, primarily in the west and midwest. His article is essentially a report on the U.S. trip, but is based as well on a review of some American publications. While we have grown accustomed in the West to reading reports on scientific forays into Russia and China, it is entertaining, in a peculiar kind of way, to have the tables thus turned. In fact, it is only as a social commentary that we can appreciate this article, because the work reported is so far out of date. If anything, we must be disappointed scientifically, for the rosy picture painted by Dr. Sedunov of weather modification research in the U.S. has now turned out to be illusory.

Principally devoted to stratus and nimbostratus clouds, the paper by Litvinov analyzes the feasibility of weather modification in parts of central Russia. It attempts to determine the possible increase in precipitation by cloud seeding under certain optimum assumptions about cloud water content and the ability to stimulate rain. Table 1, on the cloud resources available for obtaining additional precipitation, is fundamental to the paper but incomprehensible because the entries are not clearly defined. The table purports to show that the greatest potential for rain augmentation is from clouds that would normally yield no precipitation. Some discussion of cumulus clouds is given, and the author states that modification may be effected by changing the updrafts or by microphysical adjustments. He reports that a jet plane flying at a high positive pitching angle may in some conditions disperse completely in 5 minutes a cumulus cloud of 5–6 km thickness, which I find incredible. Although the overall tone of the paper is unduly optimistic, the heavy burden of uncertainty in cloud seeding experiments is occasionally revealed, as in the sentence "The introduction of additional nuclei increases the amount of precipitation, but the opposite effect is sometimes observed." As an incidental but interesting note, Fig. 1 shows that the average annual expense for snow removal in Moscow during the early 1960's was about 1.2 million rubles. This may be compared with the situation in Montreal, where for this winter the bill for salt alone was $2.5 million.

The paper by Aleksandrov is a review of instruments used for measuring condensation nuclei. It discusses thermal-diffusion and chemical-diffusion counters, as well as the more familiar expansion-chamber instruments. This is a worthy topic for review, but the paper is weakened somewhat by a number of typographical errors. For example, equation (1) has an omitted equal sign and one of the symbols in the equation is ambiguously defined.

In the text on p. 52 an important inequality is written backwards. Apart from the errors, the paper is useful. Its main conclusion is probably correct, that current instruments are inadequate to meet the requirements of modern atmospheric physics. The bibliography is especially complete, with a better balance between Russian and English references than is often the case.

Aerosol kinetics is the subject of Voloshchuk's paper, with emphasis on boundary layer aerodynamics and the inertial collection problem. The translation is less fluent than in the other papers and typographical errors abound. Most of these are insignificant, but in equations they lead to confusion. For example, equation (52) is inconsistent with (51) unless the 7 in parentheses is a misprint for 1. Included in the paper is a discussion of the washout of aerosols by cloud droplets as well as the problem of stochastic coalescence among droplets. In light of the theoretical advances in coalescence theory since 1970 this latter work can only be regarded as superficial. The subject of aerosol scavenging by cloud and rain seems to me to be treated much more thoroughly, but it is surprising that there is no mention of phoretic effects. In all, the paper usefully serves to emphasize the complexity of coagulation processes in the atmosphere.

The final contribution, a short paper by Belyaev, convincingly demonstrates the utility of intense stroboscopic illumination in studies of aerosol aspiration and collection. The streak patterns thereby produced in photographs make it possible to analyze the trajectories of individual particles, yielding more information than is obtainable by measuring only integrated effects.

Because much of the material in this book is now out of date, it can only be recommended for those who are directly concerned with the physics of aerosols and condensation nuclei. They may find the Aleksandrov survey useful, and the papers by Voloshchuk and Belyaev of some interest.

R.R. Rogers
McGill University
Montreal

ENVIRONMENTAL DATA FROM HISTORICAL DOCUMENTS BY CONTENT ANALYSIS. Manitoba Geographical Studies, No. 5, Department of Geography, The University of Manitoba, Winnipeg, 1975. 119 pp. Paperbound.

The authors describe the use of "content analysis" in general and its application in the case of a study of freeze-up and break-up dates in Hudson Bay during the last 200 years.

Content analysis and its jargon are described in great detail so that nobody, expert or not, could have any difficulty in understanding the method.

The method consist essentially in a consistent numerical expression of the verbal content of historical documents, in this case ice information from the diaries from the Hudson's Bay Company Posts. The method uses essentially only common sense, as any text interpretation does, and the long elaborations about very obvious procedures seem quite tedious at times. It is written as if the procedure should be explained to a computer, where everything has to be stated explicitly, and not to a human where a quite simplified approach is sufficient.

Although the authors claim this content analysis to be objective and scientifically reproducible, the reader will remain doubtful about these claims especially since three different text interpreters (coders), in this example, do not come to exactly the same dates of freeze-up and break-up, which is of course quite understandable. One is left with the impression that content analysis is only a modern expression for normal text interpretation, adapted in such a way that it can be used on a computer. The difficulty, however, remains that the result depends on the analyst or interpreter.

It is regrettable that the language of the authors can often be used as an example for what should not be the language in a publication. A typical case is ... "the content analysis was operationalised". ...

All these deficiencies in the shell should not distract from the real pearl inside. The authors careful examination of these unique records of climatic events over 200 years in Canada's north are immensely valuable. The publication of the yearly freeze-up and break-up dates for several localities along Hudson Bay are an invaluable set of data made available to the meteorological community. The careful endeavour of the authors to apply the same definitions of freeze-up and break-up to these historical records as are used now in the Canadian Meteorological Service is an additional and very valuable bonus. It is to be hoped that this will not be the last evaluation of these records from Hudson's Bay Company Posts for climatic history all over Northern Canada.

E. Vowinckel
McGill University
Montreal

CHEMISTRY OF THE ATMOSPHERE. Murray J. McEwan and Leon F. Phillips. Pub'd by Edward Arnold. Distributed in Canada by Macmillan Co. of Canada Ltd., 1975, 301 pp, $31.95 hardbound.

The publisher states "that this book is intended primarily as an introduction to the chemistry of the atmosphere for those with a background in chemistry or chemical physics and can be used as the basis of advanced undergraduate or graduate courses." This is true to a limited extent; it would be suitable for graduate courses in a chemistry department, but would be more suitable as a supplementary text for graduate meteorology courses in aeronomy, since it is written from a laboratory chemist's, rather than an atmospheric scientist's point of view.

Specifically, this book contains chapters on the general structure of the atmosphere, the photochemical properties of atmospheric gases, experimental techniques for atmospheric observations and laboratory measurements, composition of the chemosphere, the airglow, the ionosphere, the chemistry of polluted atmospheres and the atmosphere of other planets.

The book does have recent reviews of measurements of atmospheric constituents as well as airglow observations from rockets, balloons and aircraft. It also contains summaries of photochemical rate data for important chemical reactions appropriate to modelling the various regions of the atmosphere. It should be noted that this is a very rapidly developing field and it is difficult for any book to be current.

Notable deficiencies are the absence of chlorine chemistry in the sections on the stratosphere and a very limited discussion of tropospheric chemistry. This book is one of a number of recent books in this area and overall is a valuable addition to the developing field of atmospheric chemistry.

W.F.J. Evans
Atmospheric Environment Service
Downsview, Ontario

INFORMATION FOR AUTHORS

Editorial policy. *Atmosphere* is a medium for the publication of the results of original research, survey articles, essays and book reviews in all fields of atmospheric science. It is published quarterly by the CMS with the aid of a grant from the Canadian Government. Articles may be in either English or French. Contributors need not be members of the CMS nor need they be Canadian; foreign contributions are welcomed. All contributions will be subject to a critical review before acceptance. Because of space limitations articles should not exceed 16 printed pages and preferably should be shorter.

Manuscripts should be submitted to: the Editor, *Atmosphere*, West Isle Office Tower, 5th Floor, 2121 Trans-Canada Highway, Dorval, Quebec H9P 1J3. Three copies should be submitted, typewritten with double spacing and wide margins. Heading and sub-headings should be clearly designated. A concise, relevant and substantial abstract is required.

Tables should be prepared on separate sheets, each with concise headings.

Figures should be provided in the form of three copies of an original which should be retained by the author for later revision if required. A list of legends should be typed separately. Labelling should be made in generous size so that characters after reduction are easy to read. Line drawings should be drafted with India ink at least twice the final size on white paper or tracing cloth. Photographs (halftones) should be glossy prints at least twice the final size.

Units. The International System (SI) of metric units is preferred. Units should be abbreviated only if accompanied by numerals, e.g., '10 m', but 'several metres.'

Footnotes to the text should be avoided.

Literature citations should be indicated in the text by author and date. The list of references should be arranged alphabetically by author, and chronologically for each author, if necessary.

RENSEIGNEMENTS POUR LES AUTEURS

Politique éditoriale. *Atmosphère* est un organe de publication de résultats de recherche originale d'articles sommaires, d'essais et de critiques dans n'importe lequel domaine des sciences de l'atmosphere. Il est publié par la SMC à l'aide d'une subvention accordée par le gouvernement canadien. Les articles peuvent être en anglais ou en français. Il n'est pas nécessaire que les auteurs soient membre de la SMC; les contributions étrangères sont bien-venues. A cause des limitations d'espace les articles ne doivent pas dépasser 16 pages dans le format final. Tout article sera soumis à un critique indépendant avant d'être accepté.

Les manuscrits doivent être envoyés à : le Rédacteur, *Atmosphère*, West Isle Office Tower, 5e étage, 2121 route Trans-canadienne, Dorval, Québec H9P 1J3. Ils doivent être soumis en trois exemplaires dactylographiés à double interlignes avec de larges marges. Les titres et sous-titres doivent être clairement indiqués. Chaque article doit comporter un résumé qui soit concis, pertinent et substantiel.

Les tableaux doivent être préparés et présentés séparément accompagnés d'un titre et d'un numéro explicatifs concis.

Les graphiques doivent être présentés en trois copies dont les originaux devraient être conservés par l'auteur au cas où ils seraient nécessaire de les reviser. Une liste des légendes des graphiques doit être dactylographiée séparément. L'étiquettage doit être de grand format de façon à ce qu'il soit facilement lisible après réduction du format. Le traçage des lignes doit s'effectuer au moyen d'encre de chine en doublant, au moins, le format final, le tout sur papier blanc ou sur papier à calquer et identifié adéquatement. Les photographies (demi-teintes) devraient être présentées sur épreuves glacées au double du format final.

Les unités. Le Système International (SI) d'unités métriques est préférable. Les unités devraient être abrégées seulement lorsqu'elles sont accompagnées de nombres, ex: "10m", mais "plusieurs mètres".

Les notes de renvoie au texte doivent être évitées.

Les citations littéraires doivent être indiquées dans le texte selon l'auteur et la date. La liste des références doit être présentée dans l'ordre alphabétique, par auteur et, si nécessaire, dans l'ordre chronologique pour chaque auteur.

The Canadian Meteorological Society / La Société Météorologique du Canada

The Canadian Meteorological Society came into being on January 1, 1967, replacing the Canadian Branch of the Royal Meteorological Society, which had been established in 1940. The Society exists for the advancement of Meteorology, and membership is open to persons and organizations having an interest in Meteorology. At nine local centres of the Society, meetings are held on subjects of meteorological interest. *Atmosphere* as the scientific journal of the CMS is distributed free to all members. Each spring an annual congress is convened to serve as the National Meteorological Congress.

Correspondence regarding Society affairs should be directed to the Corresponding Secretary, Canadian Meteorological Society, c/o Dept. of Meteorology, McGill University, P.O. Box 6070, Montreal, P.Q. H3C 3G1

There are three types of membership – Member, Student Member and Sustaining Member. For 1975 the dues are $20.00, $5.00 and $60.00 (min.), respectively. The annual Institutional subscription rate for *Atmosphere* is $15.00.

Correspondence relating to CMS membership or to institutional subscriptions should be directed to the University of Toronto Press, Journals Department, 5201 Dufferin St., Downsview, Ontario, Canada, M3H 5T8. Cheques should be made payable to the University of Toronto Press.

La Société météorologique du Canada a été fondée le 1er janvier 1967, en replacement de la Division canadienne de la Société royale de météorologie, établie en 1940. Cette société existe pour le progrès de la météorologie et toute personne ou organisation qui s'intéresse à la météorologie peut en faire partie. Aux neuf centres locaux de la Société, on peut y faire des conférences sur divers sujets d'intérêt météorologique. *Atmosphere*, la revue scientifique de la SMC, est distribuée gratuitement à tous les membres. À chaque printemps, la Société organise un congrès qui sert de Congrès national de météorologie.

Toute correspondance concernant les activités de la Société devrait être adressée au Secrétaire-correspondant, Société météorologique du Canada, Département de Météorologie, l'Université McGill, C.P. 6070, Montréal, P.Q. H3C 3G1

Il y a trois types de membres: Membre, Membre-étudiant, et Membre de soutien. La cotisation est, pour 1975, de $20.00, $5.00 et $60.00 (min.) respectivement. Les Institutions peuvent souscrire à *Atmosphère* au coût de $15.00 par année.

La correspondance concernant les souscriptions au SMC ou les souscriptions des institutions doit être envoyée aux Presses de l'Université de Toronto, Département des périodiques, 5201 Dufferin St., Downsview, Ontario, Canada, M3H 5T8. Les chèques doivent être payables aux Presses de l'Université de Toronto.